REMOVAL OF HEXAVALENT CHROMIUM FROM WASTEWATER USING MODIFIED MULTIWALL CARBON NANOTUBES

by

Tamara Georgesaleh Dokmaji

A Thesis Presented to the Faculty of
American University of Sharjah
College of Engineering
in Partial Fulfillment
of the Requirements
for the Degree of

Master of Science in
Chemical Engineering

Sharjah, United Arab Emirates

December 2018

Approval Signatures

We, the undersigned, approve the Master's Thesis of Tamara Georgesaleh Dokmaji

Thesis Title: Removal of Hexavalent Chromium from Wastewater using Modified Multiwall Carbon Nanotubes

Signature	**Date of Signature** (dd/mm/yyyy)
_____	_____
Dr. Taleb Ibrahim Professor, Department of Chemical Engineering Thesis Advisor	
_____	_____
Dr. Mustafa Khamis Professor, Department of Biology, Chemistry and Environmental Sciences Thesis Co-Advisor	
_____	_____
Dr. Zarook Shareefdeen Professor, Department of Chemical Engineering Thesis Committee Member	
_____	_____
Dr. Mohamed Abouleish Associate Professor, Department of Biology, Chemistry and Environmental Sciences Thesis Committee Member	
_____	_____
Dr. Naif Darwish Head, Department of Chemical Engineering	
_____	_____
Dr. Ghaleb Husseini Associate Dean for Graduate Affairs and Research College of Engineering	
_____	_____
Dr. Richard Schoephoerster Dean, College of Engineering	
_____	_____
Dr. Mohamed El-Tarhuni Vice Provost for Graduate Studies	

Acknowledgement

I would like to thank my advisors Dr. Taleb Ibrahim and Dr. Mustafa Khamis for providing me with complete guidance, encouragement and mentorship during my work in this thesis. This work marks the start of my journey in the field of research and I look forward to expanding my knowledge in more areas. I am very thankful to the Chemical Engineering Department at the American University of Sharjah for providing me with the technical engineering background and skills to complete this research.

Also, I highly appreciate the Department of Biology, Chemistry and Environmental Sciences for permitting the use of their well-established laboratories during my experimental research for this study. In addition, I would like to thank Mr. Ziad Sara and Mr. Nedal Abu-Farha for their nonstop support and assistance.

Last of all, I would like to acknowledge the unconditional care and love from my family and friends during my academic life and beyond.

Dedication

To My Sister, My Brother, My One and Only Father and Mother…

Abstract

Recently, the interest and research on the removal of heavy metals from wastewater have dramatically increased due to the adverse effects they have on humans, flora and fauna. Chromium, which is a heavy metal, is the tenth most abundant element in the universe and naturally occurs in the form of hexavalent chromium [Cr(VI)] and trivalent chromium [Cr(III)]. In this thesis, an adsorption technique using modified multiwall carbon nanotubes (MWCNTs) is investigated for Cr(VI) removal from wastewater. The surface of the MWCNTs was modified with a cationic surfactant, cetyl trimethylammonium bromide (CTAB). Surface characterization was conducted using Fourier Transform Infrared spectroscopy (FTIR), Thermal Gravimetric Analyzer (TGA), Scanning Electron Microscope (SEM), and Energy Dispersive X-ray Spectroscope (EDS) in which a thorough review of results revealed that MWCNTs modification with CTAB was successful. The optimum conditions for adsorption using MWCNTs-CTAB were determined. The optimum values in terms of adsorbent dosage, contact time, pH, and temperature were found to be 0.05 g, 25 min, 4.5, and 25 ^{o}C, respectively. Fitting equilibrium data using various isotherm models revealed that the adsorption of Cr(VI) on MWCNTs-CTAB follows a Langmuir isotherm model with maximum adsorption capacity of 27.78 mg/g and Langmuir adsorption capacity of 3.956 L/mg. In addition, kinetic parameters were also fitted on several models and the data revealed that MWCNTs-CTAB followed a pseudo- second order reaction model with rate constant $9.85*10^{-4}$ g/mg.min. A thermodynamic study showed that the proposed adsorption process is spontaneous, endothermic and the mode of adsorption is physisorption with Gibbs free energy of -1.3 kJ/mol at 25 ^{o}C. From this batch experimental study, it can be concluded that the removal of Cr(VI) from wastewater using MWCNTs-CTAB was successful and a removal efficiency of 98% was achieved at the selected optimum conditions.

Search Terms: Multiwall carbon nanotubes; cetyl trimethylammonium bromide; hexavalent chromium; adsorption, isotherm models, kinetic

Table of Contents

Abstract 6
List of Figures 10
List of Tables 12
Nomenclatures 13
Chapter 1. Introduction 17
1.1. Overview. 17
1.2. Research Objective. 17
1.3. Research Contribution. 18
1.4. Thesis Organization. 18
Chapter 2. Background and Literature Review 19
2.1. Overview of Heavy Metals. 19
2.2. Sources of Heavy Metals. 19
2.3. Adverse Effects of Heavy Metals. 19
2.3.1. Effect of heavy metals on soil and plant. 20
2.3.2. Effects on aquatic environment. 20
2.3.3. Effects on human health. 21
2.4. Heavy Metals Laws and Regulations. 21
2.5. Chromium. 23
2.6. Techniques used for the Removal of Chromium from Wastewater. 24
2.6.1. Chemical precipitation. 25
2.6.2. Ion exchange. 25
2.6.3. Coagulation and flocculation. 26
2.6.4. Membrane filtration. 27
2.6.4.1. Ultrafiltration (UF). 27
2.6.4.2. Nanofiltration (NF). 27
2.6.4.3. Reverse osmosis (RO). 28
2.6.5. Electro dialysis (ED). 28
2.6.6. Membrane electrolysis (ME). 29
2.6.7. Electrochemical precipitation (ECP). 29
2.6.8. Adsorption. 29
2.7. Overview of Adsorption. 30
2.7.1. Adsorption equilibrium. 32
2.7.1.1. Langmuir isotherm. 33
2.7.1.2. Freundlich isotherm. 34
2.7.1.3. Dubinin-radushkevich (D-R) isotherm. 34
2.7.1.4. Temkin isotherm. 35
2.7.1.5. Sips isotherm. 35

2.7.2. Adsorption kinetic models. 36
2.7.2.1. Pseudo- first order. 36
2.7.2.2. Pseudo- second order. 36
2.7.2.3. Elovich reaction model. 36
2.7.3. Adsorption mechanism. 36
2.7.3.1. Film diffusion. 37
2.7.3.2. Intraparticle diffusion. 37
2.7.4. Adsorption thermodynamics. 37
2.8. Adsorbents. 38
2.8.1. Carbon nanotubes (CNTs). 40
2.8.2. CNTs synthesis. 41
2.8.2.1. Electric arc-discharge. 42
2.8.2.2. Laser ablation. 42
2.8.2.3. Chemical vapor deposition (CVD). 42
2.8.2.4. Hydrothermal. 43
2.8.3. CNTs properties and applications. 43
2.8.4. CNTs functionalization. 45
2.8.5. Studies of CNTs for removal of heavy metals from wastewater. 46
Chapter 3. Materials and Methods 49
3.1. Materials. 49
3.2. Instrumentation. 49
3.3. Methods. 50
3.3.1. Adsorption experiment. 50
3.3.2. Quality assurance method. 50
3.3.3. Surface modification. 51
3.3.4. Regeneration. 51
Chapter 4. Results and Discussion 52
4.1. Surface Characterization. 52
4.1.1. TGA. 52
4.1.2. FTIR. 52
4.1.3. Surface area analysis. 54
4.1.4. SEM. 55
4.1.5. EDS. 55
4.2. Quality Assurance Results. 55
4.3. Adsorption Parameters Optimization. 58
4.3.1. Effect of adsorbents dosage. 58
4.3.2. Effect of pH. 58

4.3.3. Effect of contact time. 59
4.3.4. Effect of temperature. 60
4.4. Adsorption Equilibrium Isotherms. 61
4.4.1. Langmuir isotherm model. 63
4.4.2. Freundlich isotherm model. 63
4.4.3. Temkin isotherm model. 63
4.4.4. Dubinin–Radushkevich (D-R) isotherm model. 64
4.4.5. Sips isotherm model. 65
4.5. Adsorption Kinetics. 66
4.6. Adsorption Mechanism. 68
4.7. Adsorption Thermodynamics. 71
4.8. Regeneration. 71
Chapter 5. Conclusions and Recommendations 74
References 76
Vita 86

List of Figures

Figure 2.1: Relative distribution of Cr(VI) species in water as a function of pH and concentration 24
Figure 2.2: Schematic of mass transfer in adsorption process 32
Figure 2.3: Structures of a) SWCNTs and b) MWCNTs 41
Figure 4.1: TGA results showing weight loss (%) versus temperature (°C) for CTAB, raw MWCNTs, modified MWCNTs with CTAB. 52
Figure 4.2a: FTIR results of raw MWCNTs (top), MWCNTs-CTAB (middle), CTAB (bottom) 53
Figure 4.2b: FTIR result of MWCNTs-CTAB (top) before adsorption of Cr(VI) and FTIR result of MWCNTs-CTAB Cr(VI) (bottom) after Cr(VI) adsorption 54
Figure 4.3: SEM result images (a) raw MWCNTs, (b) MWCNTs-CTAB, (c) MWCNTs-CTAB after adsorption of Cr(VI), (d) MWCNTs-CTAB-Cr(VI) after regeneration using KCl at 25 °C 56
Figure 4.4: EDS analysis of (a) raw MWCNTs, (b) MWCNTs-CTAB, (c) MWCNTs-CTAB after adsorption of Cr(VI) 57
Figure 4.5: Effect of adsorbent dosage on the removal of Cr(VI) from aqueous solution for MWCNTs-CTAB at contact time = 120 min, pH = 2 ± 0.05, temperature = 25 ± 2 °C, initial concentration = 100 ppm and shaking rate = 150 rpm. 58
Figure 4.6: Effect of pH on the removal of Cr(VI) from aqueous solution for MWCNTs-CTAB at contact time = 120 min, initial concentration = 100 ppm, temperature = 25 ± 2 °C, adsorbent dosage = 0.05 g, and shaking rate = 150 rpm. 59
Figure 4.7: Effect of contact time on the removal of Cr(VI) from aqueous solution for MWCNTs-CTAB at pH = 4.5, initial concentration = 100 ppm, temperature = 25 °C, adsorbent dosage = 0.05 g, and shaking rate = 150 rpm. 60
Figure 4.8: Effect of temperature on the removal of Cr(VI) from aqueous solution for MWCNTs-CTAB at pH = 4.5 ± 0.05, initial concentration= 100 ppm, contact time = 30 min, adsorbent dosage = 0.05 g, and shaking rate = 150 rpm. 61
Figure 4.9: Change in removal efficiency with initial concentration using MWCNTs-CTAB, at adsorbent dosage = 0.05 g, contact time = 30 min, pH = 4.5 ± 0.05, temperature = 25 ± 2 °C and shaking time = 150 rpm 62
Figure 4.10: Change in adsorption capacity with initial concentration using MWCNTs-CTAB at adsorbent dosage = 0.05 g, contact time = 30 min, pH = 4.5 ± 0.04, temperature= 25 ± 2 °C and shaking time = 150 rpm 63
Figure 4.11: Langmuir isotherm model for adsorption of Cr(VI) on MWCNTs-CTAB 64
Figure 4.12: Freundlich isotherm model for adsorption of Cr(VI) using MWCNTs-CTAB 64
Figure 4.13: Temkin isotherm model for adsorption of Cr(VI) using MWCNTs-CTAB 65
Figure 4.14: D-R isotherm model for adsorption of Cr(VI) using MWCNTs-CTAB. 65
Figure 4.15: Sips isotherm model for adsorption of Cr(VI) using MWCNTs-CTAB. 66
Figure 4.16: Pseudo- first order model for adsorption of Cr(VI) using MWCNTs-CTAB 68

Figure 4.17: Pseudo- second order model for adsorption of Cr(VI) using MWCNTs-CTAB 69
Figure 4.18: Elovich model for adsorption of Cr(VI) using MWCNTs-CTAB 70
Figure 4.19: Intraparticle diffusion model for Cr(VI) adsorption using MWCNTs-CTAB 70
Figure 4.20: Film diffusion model for Cr(VI) adsorption using MWCNTs-CTAB .. 70
Figure 4.21: Van't Hoff plot of LnK_e versus 1/T for the adsorption of Cr(VI) using MWCNTs-CTAB 71
Figure 4.22: Removal efficiencies of Cr(VI) using regenerated MWCNTs-CTAB at regeneration temperature = 25 ± 2 ^oC and regeneration solution = 0.1 M KCl. Adsorption cycle 1 & 2 were at pH = 4.5 ± 0.05, initial concentration = 100ppm, contact time = 30 min, adsorbent dosage = 0.5 g, and shaking rate = 150 rpm 72
Figure 4.23: Removal efficiencies of Cr(VI) using regenerated MWCNTs-CTAB at regeneration temperature = 35 ± 2 ^oC and regeneration solution = 0.1 M KCl. Adsorption cycle 1 & 2 were at pH = 4.5 ± 0.05, initial concentration = 100 ppm, contact time = 30 min, adsorbent dosage = 0.5 g, and shaking rate = 150 rpm 73

List of Tables

Table 2.1: Common applications of common heavy metals 20
Table 2.2: Heavy metals and its associated LD50 metals 21
Table 2.3: Common health effects of common heavy metals 22
Table 2.4: Examples of few heavy metal's permissible limits by EPA Regulations and WHO Guidelines 23
Table 2.5: Summary of various techniques used to remove heavy metals from wastewater 30
Table 2.6: Adsorption capacity of adsorbents for heavy metals in solution 39
Table 2.7: Examples of non-conventional adsorbents 39
Table 2.8: CNT synthesis methods, products, advantages and disadvantages 45
Table 4.1: Summary of FTIR peaks of the regenerated samples 54
Table 4.2: Surface area results for raw MWCNTs and MWCNTs-CTAB 55
Table 4.3: Adsorption isotherm parameters for the five models for Cr(VI) removal using MWCNTs-CTAB 67
Table 4.4: Various functional groups MWCNTs adsorption capacities 67
Table 4.5: Adsorption Kinetics Model Parameters 67
Table 4.6: Thermodynamic parameters fitted to Sips Equation 71

Nomenclatures

Acronyms

ATP	Adenosine Triphosphate
BC	Before Christ
CNTs	Carbon Nanotubes
Cr(III)	Trivalent Chromium
Cr(VI)	Hexavalent Chromium
CTAB	Cetyl Trimethylammonium Bromide
CVD	Chemical Vapor Deposition
DNA	Deoxyribonucleic Acid
D_p	Pore diffusion
D-R	Dubinin-Radushkevich
D_s	Surface diffusion
ECP	Electrochemical Precipitation
ED	Electro Dialysis
EDS	Energy Dispersive X-ray Spectroscopy
EMT	External Mass Transfer
EPA	Environmental Protection Act
FTIR	Fourier Transform Infrared Spectroscopy
GAC	Granulated Activated Carbon
IARC	International Agency for Research on Cancer
IMT	Internal Mass Transfer
IUPAC	International Union of Pure and Applied Chemistry
LD50	Lethal Dosage to kill 50% of tested species
MCL	Maximum Contamination Level
MCLG	Maximum Contamination Limit Goal
ME	Membrane Electrolysis

MWCNTs	Multiwall Carbon Nanotubes
NASA	National Aeronautics and Space Administration
Nd:YAG	Neodymium-Doped Yttrium-Aluminum-Garnet
NF	Nanofiltration
NIOSH	National Institute for Occupational Safety and Health
NPs	Nanoparticles
PAC	Polyaluminium chloride
PAM	Polyacrylamide
PFS	Polyferricsulfate
ppb	Parts per billion
ppm	Parts per million
RO	Reverse Osmosis
SEM	Scanning Electron Microscopy
SSE	Sum of Square Errors
SWCNTs	Single Wall Carbon Nanotubes
TGA	Thermogravimetric Analysis
UF	Ultrafiltration
UV-VIS	Ultraviolet Visible Spectroscopy
WHO	World Health Organization

Notations

A_T	Temkin isotherm equilibrium binding constant (L/g)
b_T	Temkin isotherm constant
B	D-R heat of sorption constant (J/mol)
C	Film diffusion constant for thickness of the boundary layer
C_b	Bulk concentration(mg/L)
C_e	Equilibrium concentration (mg/L)

C_{id}	Film diffusion constant for thickness of the boundary layer
C_o	Initial concentration (mg/L)
G	Free energy (kJ/mol)
H	Enthalpy (kJ/mol)
K_{L}	Langmuir adsorption constant (L/mg).
K_{ad}	D-R isotherm constant (mol^2/kJ^2)
K_e	Equilibrium constant
K_f	Freundlich adsorption capacity parameter (L/mg)
k_1	Pseudo- first order adsorption rate constant (min^{-1})
k_2	Pseudo- second order adsorption rate constant (g/mg.min)
k_{fd}	Film diffusion rate constant (min^{-1})
k_{id}	Intraparticle diffusion rate constant ($mg/g.min^{0.5}$)
M	Mass of adsorbent (g).
n	Freundlich adsorption intensity parameter
n_s	Sips constant
Q_m	Maximum monolayer adsorption capacity (mg/g),
R	Universal gas constant (8.314 J/mol.K)
R_L	Langmuir dimensionless parameter
S	Entropy (kJ/mol.K)
t	Contact time (min)
T	Temperature (K)
q_e	Adsorbent loading at equilibrium (mg/g)
q_s	Theoretical isotherm saturation capacity (mg/g)
q_t	Adsorbent loading at time t (mg/g)
q_{th}^e	Theoretical maximum adsorption capacity (mg/g)
V	Volume of aqueous solution (L)

Greek Symbols

Δ	Change or difference in certain quantity
β	Desorption adsorption constant (g/mg)
ε	D-R isotherm constant
$\propto$	Initial adsorption rate (mg/g.min)
Φ	Porosity

Chapter 1. Introduction

1.1. Overview

With two hundred years of industrial revolution, the generation of contaminated wastewaters has dramatically increased causing detrimental impacts on the environment. Therefore, laws and regulations have been implemented on dischargers to limit and force wastewater treatment [1]. Additionally, in parts of the world where there is a shortage of clean fresh water, wastewater treatment has become a necessity [2]. In general, the objective of wastewater treatment is to allow effluents from humans and industries to be disposed in a sustainable manner without endangering the human health or the environment. The goal is to dispose wastewater safely and be able to reuse it in a practical manner [3]. Wastewater contamination from industries can come from oil extractions, refinery waste, heavy metals, and thermal and process by-products [2]. Contamination of wastewater by the toxic heavy metal, hexavalent chromium [Cr(VI)], is the focus of this study. Chromium is the 10th most abundant element in the universe and Cr(VI) is categorized as a carcinogenic heavy metal to humans. Chromium is usually discharged into water bodies from industries related to metal plating, paints and pigments, leather tanning, textile dyeing, printing inks and wood preservation, where all contributors are faced to comply with the adopted discharge limits of chromium in their respective region [4]. For example, according to the Regulation and Supervision Bureau for the water, wastewater and electricity sector in the Emirate of Abu Dhabi the maximum contamination limit (MCL) of total chromium discharged into sewerage system from any industrial, commercial, agricultural, medical, scientific or trade activity excluding domestic wastewater is not to exceed 5 mg/L.

1.2. Research Objective

Pressured by the strict discharge laws and regulations of chromium and the acknowledgment of the adverse effects it has on humans, animals and environment. This thesis is aimed to investigate the efficacy of surface modified MWCNTs as a potential adsorbent to remove Cr(VI) from wastewater. Surface characteristics of MWCNTs modified with the surfactant cetyl trimethylammonium bromide (CTAB) are obtained.

1.3. Research Contribution

This thesis is aimed to contribute in wastewater treatment field of research where batch experimental studies are used to obtain the optimal parameters for efficient adsorption of Cr(VI) from wastewater using modified MWCNTs. The adsorption parameters which are assessed for Cr(VI) removal are adsorbent dosage, pH, removal efficiency, initial concentration, contact time and temperature.

1.4. Thesis Organization

Following this chapter, this thesis is organized as follows; Chapter 2 provides an overview of the different heavy metals and their common sources of occurrence and adverse effects. It also focuses on chromium as the selected heavy metal for this study. Chapter 2 provides examples of common techniques usually used for wastewater treatment. It highlights adsorption as the selected treatment technique and details the different factors, which play an important role in adsorption modeling, such as isotherm models and kinetic models. Lastly, the chapter defines various adsorbents and focuses on carbon nanotubes (CNTs) and their synthesis, functionalization and applications. Chapter 3 covers the acquired experimental techniques used during this study; including materials, instrumentations and methods. Chapter 4 highlights and discusses the experimental results for the adsorption of Cr(VI) using MWCNTs-CTAB. Finally, Chapter 5 concludes this study and highlights the key findings and recommendations.

Chapter 2. Background and Literature Review

2.1. Overview of Heavy Metals

Heavy metals are natural components of the Earth's crust. However, contamination from heavy metals can be due to industrial and/or consumer discharges to fresh waters and from the surrounding environment. Heavy metals have become a concern to the society because they cannot be degraded or destroyed and tend to bioaccumulate in environment and human bodies. They can enter and concentrate in human bodies through food and water consumption, by which they can cause various adverse effects [1]. For example, heavy metals can impair mental and neurological systems by manipulating neurotransmitter production and functions [1]. Heavy metals can be found in various manufacturing industries such as pigments and paints, textiles, fertilizers, electronics, metal hardening, tanning, rubber, and copper plating [5]. However, not all heavy metals are toxic. In small concentration, they can serve as trace minerals essential for humans' every day function. For example, calcium, phosphorus and sodium are all essential nutrients for bone and teeth structure; in addition, copper, zinc, and iron are all vital components for blood and function of enzymes [6].

2.2. Sources of Heavy Metals

The use of heavy metals in manufacturing industries is very common. The type and quantity of heavy metals used depend on the type of industry, laws and regulations, and quantity of process flows [7]. Chromium, copper, lead and cadmium are some of the widely used heavy metals [4, 7, 8]. Hexavalent chromium [Cr(VI)] is generally used in metal plating industries, as a corrosion inhibitor in cooling towers, tanning reagent in leather industries and also in the manufacturing of paints, dyes and explosives [7]. Trivalent chromium [Cr(III)] is less frequently used but can be found in ceramic, glass and textile industries. Table 2.1 summaries some heavy metals and their relevant applications in industries.

2.3. Adverse Effects of Heavy Metals

In trace amounts, heavy metals are an essential component to maintain various biological and physiological functions in living organisms [9]. However, they become harmful when their concentration exceeds the threshold. Heavy metals are known for their adverse health effects where their exposure is increasing in many parts of the world. Heavy metals are significant environmental contaminants which have a harmful

effect on ecological, evolutionary, nutritional and environmental processes [9]. For instance, acid rain can leach through the soil and release heavy metals into streams, lakes, rivers, and groundwater [5]. Most common heavy metals in wastewater include arsenic, cadmium, chromium, copper, lead, nickel, and zinc, all of which cause risks for human health and the environment [9]. The following subsections discuss the effects of heavy metals on the environment and human health.

Table 2.1: Common applications of common heavy metals

Heavy metal	Application	References
Mercury	Electrical switches, florescent light bulb; preservatives; medications; discharge from refineries and factories; runoff from landfills and croplands	[10, 11, 12]
Lead	Automobile battery; weather and sound proofing building; water pipes and ducts; roofing flashing, corrosion of household plumbing systems	[10, 11]
Cadmium	Nicad battery; pigment; smelters; corrosion of galvanized pipes; discharge from metal refineries; runoff from waste batteries and paints	[10, 11, 12]
Arsenic	Pesticide; production of iron; steel mining; runoff from orchards, runoff from glass & electronics production wastes	[10, 11]
Cr(VI)	Electroplating; corrosion protection leather tanning; metal plating industries; discharge from steel and pulp mills	[10, 11, 12]
Nickel	Electroplating industry and pharma sector	[12]
Zinc	Model rockets	[11, 12]

2.3.1. Effect of heavy metals on soil and plant. Heavy metals are one of the major contributors to soil pollution, where they can disturb the microbial activity and structure of the soil [5]. Common heavy metals found in soil are copper, nickel, zinc, and chromium. Heavy metals can be found in fertilizers used to increase production yield, these fertilizers get absorbed into plants' roots and affect plants' and soil structure. Consequently, these metals can cause plant chlorosis, weak plant growth, yield depression, and may even reduce nutrient uptake of the plants [5]. Properties such as pH, organic matter, and clay content can define the extent of heavy metal pollution in soil.

2.3.2. Effects on aquatic environment. Heavy metals in aquatic environment are highly persistent, poisonous, even in small amounts, and can cause

oxidative stresses. The presence of heavy metals in aquatic environment can also be transferred up the food hierarchy through consumption [5, 13]. Table 2.2 provides an example of the fatal characteristics of heavy metals by providing the lethal dosage (LD50) of various heavy metals found in aquatic environment. LD50 is the concentration of heavy metal required to kill 50% of the tested aquatic species; however, environmental conditions such as temperature, pH, and water hardness will affect the toxicity amongst the different tested heavy metals [13].

Table 2.2: Heavy metals and its associated LD50 metals [13]

Heavy Metal	Affected species	Concentration (mg/L)
Cadmium	Common carp	22
Chromium	Brook trout	59
Lead	Brook trout	3.4
Nickel	Rainbow trout	45

2.3.3. Effects on human health. Effects of heavy metals on humans depend on their concentration and toxicity level. For example, cadmium can cause serious problems in the liver, kidneys, lungs, placenta, brain and bones [5, 13]. High levels of cadmium may lead to pulmonary edema and even death [5]. In addition, high concentrations of zinc can cause impairment of growth and reproduction [5]. Conversely, it has been found that lead, even in small concentrations, can cause kidney and liver damage, disrupt reproduction and central nervous system functions, and may eventually cause death [5]. Lastly, arsenic is considered to be carcinogenic in all its oxidation states and it can form complexes and coenzymes which prevent the production of adenosine triphosphate (ATP) during respiration [5]. Table 2.3 summarizes the adverse health effects of some heavy metals on humans.

2.4. Heavy Metals Laws and Regulations

Laws and Regulations on heavy metals discharge have been established to protect the environment from their adverse effects by controlling the amount of heavy metals discharged from industries and humans. Toxic heavy metals found in wastewater discharges can be in the form of metal ions and salts [10]. Heavy metals within the European Union are defined under the ‘framework’ Dangerous Substances Directive (76/464/EEC), which categorizes heavy metals into two categories; black and grey lists. The black list contains cadmium and mercury which are considered very toxic, hard to degrade and can easily bioaccumulate [13]. While, the grey list contains heavy metals

which are environmentally harmful but to a lesser extent when compared to the black list. The grey list includes chromium, copper, zinc, nickel and lead [13].

Table 2.3: Common health effects of common heavy metals

Heavy metal	Health Effects	References
Mercury	Central nervous system, kidney damage	[10, 11, 12]
Lead	Deterioration of bones, dental cavities, increase blood pressures. On infants and children: delays in physical or mental development; children could show slight deficits in attention span and learning abilities	[10, 11]
Cadmium	Liver and kidney failure, Carcinogenic, causes lung fibrosis, dyspnoea and weight loss	[10, 11, 12]
Arsenic	Vomiting, diarrhea, liver damage, diabetes, lung cancer; skin damage or problems with circulatory systems	[10, 11]
Cr(VI)	Weak immune system, allergic dermatitis, suspected human carcinogen, producing lung tumors, allergic dermatitis	[10, 11, 12]
Nickel	Neurological deficits, developmental deficits in childhood, high blood pressure, Causes chronic bronchitis; reduced lung function; cancer of lungs and nasal sinus	[12]
Zinc	Causes short-term illness called “metal fume fever” and restlessness	[11, 12]

To protect against such kinds of toxic heavy metals, international organizations such as Environmental Protection Act (EPA), European Union Commission and World Health Organization (WHO) have set limitations for the concentration of heavy metals in drinking water [13]. EPA and WHO have defined two terms to control and regulate heavy metals discharges. These terms are, maximum contamination level (MCL) and maximum contamination limit goal (MCLG). MCL is the maximum allowed level of heavy metals in drinking water while, and MCLG is the non-enforceable level of heavy metals where no risk to health is expected. Table 2.4 summarizes the EPA and WHO recommended limits of some heavy metals for safe drinking water.

Table 2.4: Examples of few heavy metal's permissible limits by EPA Regulations and WHO Guidelines

Heavy Metals	EPA Regulation (mg/L)		WHO Guidelines (mg/L)	References
	MCLG	MCL		
Arsenic	0	0.01	0.01	[14, 15]
Cadmium	0.005	0.005	0.003	
Cr(VI)	0.1	0.1	0.05	
Copper	1.3	1.3	2	
Cyanide	0.2	0.2	0.07	
Fluoride	4	4	1.5	
Lead	0	0.015	0.01	
Mercury	0.002	0.002	0.001	

2.5. Chromium

There are various heavy metals which have carcinogenic and toxic properties as discussed in the sections above these include arsenic, cadmium, chromium, lead, and mercury. In this study, Chromium is selected as the heavy metal to be removed from wastewater. Chromium is categorized in the grey heavy metals' list. It is the tenth most abundant element in the universe and exists naturally in the environment in the form of Cr(III) and Cr(VI). However, chromium has various oxidation states ranging from −4 to +6, where +3 state is most stable energetically. The oxidation states +1, +2, +4 and +5 are relatively rare and oxidation states −4, −3, −2, −1 and 0 are very rare [16]. Cr(VI) is known to have strong oxidizing properties which is a function of pH and this property deems it toxic to plants and animals [17]. It can easily penetrate the cell membrane and oxidize biological molecules. Cr(VI) also has corrosive properties and in humans it can cause severe gastric damage, liver, kidney and lung cancer and other health related complications [4]. On the contrary, Cr(III) is an essential element for humans' glucose and protein metabolism [18]. Cr(III) is relatively less toxic and in trace amounts it does not impose problems to the environment [4]. This study will focus on the removal of Cr(VI) from wastewater due to its toxic properties in comparison to Cr(III).

Cr(VI) is categorized as a group 1 carcinogen for humans by the International Agency for Research on Cancer (IARC). It has a MCL of 0.1 mg/L and 0.05 mg/L based on EPA and WHO standards, respectively (Table 2.3). The National Institute for Occupational Safety and Health (NIOSH) has even recommended that the amount of

chromium in water be limited to 0.001 mg/m^3 [19]. The Regulation and Supervision Bureau for the water, wastewater and electricity sector in the Emirate of Abu Dhabi had set the MCL of total chromium discharged into sewerage system from any industrial, commercial, agricultural, medical, scientific or trade activity excluding domestic wastewater to a maximum 5 mg/L [20]. Abu Dhabi Quality and Conformity Council (ADS 23/2017) have assigned a MCL for chromium discharged into marine environment to be 0.2 mg/L for total chromium and 0.15 mg/L for Cr(VI) [21].

The form in which Cr(VI) is present in wastewater is dependent on the pH and concentration of Cr(VI) as demonstrated in Figure 2.1. Cr(VI) can be in the form of chromic acid (H_2CrO_4) and its salts, hydrogen chromate ion ($HCrO_4^-$), chromate ion (CrO_4^{2-}) and dichromate ($Cr_2O_7^{2-}$). The predominant species present at a pH less than 1 are H_2CrO_4, and at a pH of 1 to 6 are $HCrO_4^-$ and $Cr_2O_7^{2-}$. CrO_4^{2-} is expected at pH values above 6. Dichromate ion ($Cr_2O_4^{2-}$) is a dimer of $HCrO_4^-$, less a water molecule, which forms when the concentration of chromium exceeds 1 g/L approximately [17].

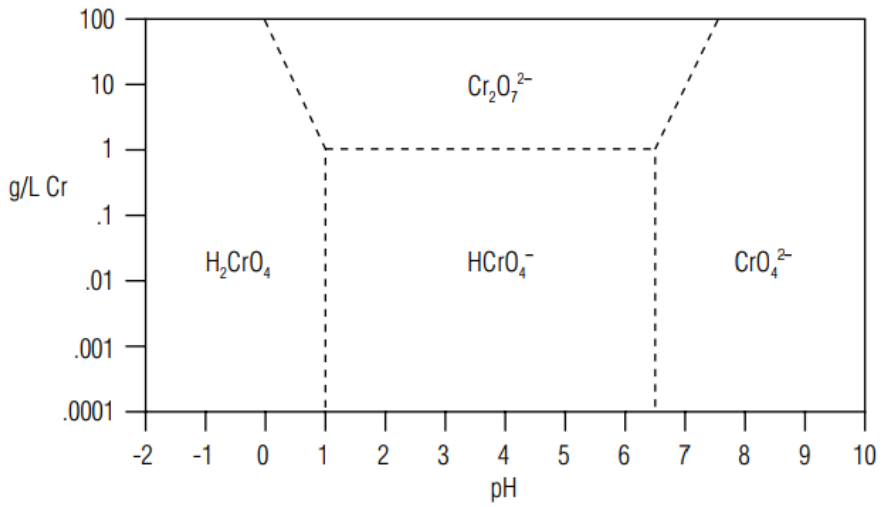

Figure 2.1: Relative distribution of Cr(VI) species in water as a function of pH and concentration [17]

2.6. Techniques Used for the Removal of Chromium from Wastewater

Treatment of wastewater contaminated with heavy metals is an essential step prior to water disposal due to strict laws and regulations and their environmental impacts. The intensity of the water treatment is variant as it is heavily dependent on the purpose of product. Therefore, the type of treatment process or combination of processes used will depend on the metal(s) to be removed and the ultimate concentration required. In the subsections below, brief introduction of the typical

techniques used for heavy metal removal are discussed along with the advantages and disadvantages of each method. The selected process for this study is mainly dependent on pH, chemical usage, initial feed concentration, energy requirement and capital and operational costs [13, 8].

2.6.1. Chemical precipitation. Chemical precipitation is a process which is commonly used due to its low operating cost and simplicity. In this process, a chemical reagent is used to react with the heavy metal ions to form insoluble precipitates. The precipitates are then removed using sedimentation or filtration technique. The effluent can then be further treated or directly discharged to the environment. The most common chemical precipitation techniques are hydroxide and sulfide precipitation [22]. Hydroxide precipitation process is a widely used technique due to its simplicity, ease of pH control and lower cost. A pH in the range of 8 - 11 would be optimal for metal hydroxide precipitates [22]. This process uses coagulants to enhance heavy metal removal; common coagulants used are alum, lime, iron salts, and organic polymers. It has been reported that alum and lime are usually used to remove Cr(VI) from wastewater. A drawback of this technique is the large production of low-density sludge which requires dewatering prior to disposal. Another drawback is that in mixed effluent feed, an optimum pH for the removal of one metal may lead the other metal to dissolve back into the solution [22]. Furthermore, sulfide precipitation process provides a large difference in solubility in comparison to the hydroxide technique. This process can achieve a high degree of metal precipitation on a wide range of pH [22]. Drawback of this technique is that toxic hydrogen sulfide fumes can be produced in acidic conditions, and therefore precipitation process is best practiced in neutral or basic pH ranges. An additional drawback of this process is that clumps formed can hinder the settling or filtration process. Both hydroxide and sulfide precipitation techniques require excessive amounts of chemicals, long residence time, and slow precipitation process [22, 23].

2.6.2. Ion exchange. Ion exchange is a technique usually used to remove calcium or magnesium metals from wastewater [23, 24]. Ion exchange is characterized to be capable of handling high capacity feed, provide high removal efficiency and require short residence time [22]. This technique uses synthetic or natural resins where exchange of either cations or anions takes place within the feed [22]. Synthetic resins,

natural zeolites and naturally occurring silicate minerals, have been widely used to remove heavy metals from aqueous solutions due to their low cost, high removal efficiency and high abundance [22]. The removed heavy metals can be recovered through electrolytic recovery. This technique requires an electric current to be passed through an aqueous metal-bearing solution containing a cathode plate and an insoluble anode, where positively charged metallic ions cling to the negatively charged cathodes leaving behind a metal deposit that is strippable and recoverable [23]. Common cation exchanger resins include sulfonic acid groups for highly acidic resins and carboxylic acid groups for weak acidic resins. The hydrogen ions present in the resin serve as exchangeable ions with metal cations [22]. Factors such as pH, temperature, initial metal concentration and contact time can affect the treatment process. Drawbacks of this process is that, this system is prone to fouling at highly concentrated feed, non-selective and highly pH sensitive [23]. In addition, corrosion is a significant problem where electrodes would frequently have need to be replaced [23].

2.6.3. Coagulation and flocculation. Coagulation and flocculation are another process used to treat wastewater contaminated with heavy metals [22, 24]. Coagulation is a process of destabilization of colloidal particles by adding a coagulant reagent which acts to neutralize and overcome any repulsive forces between the particles [22, 24]. Most common coagulants used in wastewater treatment are aluminum, ferrous sulfate and ferric chloride which act by forming amorphous metal hydroxide precipitates of the colloidal particles [22]. Flocculation is a process which follows the coagulation process in which large agglomerates form by adding a polymer to bind the particles together. Once larger particles are found, they can be removed or separated by filtration, straining or sedimentation. Common flocculants used are polyaluminium chloride (PAC), polyferricsulfate (PFS) and polyacrylamide (PAM). However, removal of heavy metals from wastewater using these flocculants is inefficient and impractical [22]. In common practice, coagulation and flocculation can treat inorganic effluent with a metal concentration of less than 100 mg/L or higher than 1,000 mg/L and it is suitable at a pH range of 11.0 to 11.5. Drawbacks of using this process is that it requires high operational cost, which is due to large chemical consumption and chemical dependency. In addition, this process generates large

amount of toxic sludge, which require stabilization prior to disposal to prevent heavy metals from leaching into the environment [25].

2.6.4. Membrane filtration. Membrane filtration is a widely used process to remove heavy metals, suspended solids and organic compounds. Membrane filtration offers high removal efficiency, simple operation and requires relatively small space. Membrane filtration is generally coupled with a backwashing process or a chemical cleaning process to remove contaminants accumulated on the membrane during filtration. During backwash, flow direction is reverse for 30 seconds to 3 minutes and the accumulated contaminants are detached from the membrane. Chemical cleaning is particularly used to remove inorganic and organic accumulations that are not removed during backwash [26]. There are various types and techniques used in membrane filtration which are dependent on the size of particle to be removed. Common membranes types used for wastewater treatment are ultrafiltration (UF), nanofiltration (NF) and reverse osmosis (RO) [25].

2.6.4.1. *Ultrafiltration (UF).* UF process uses a permeable membrane to separate heavy metals, macromolecules and suspended solids from inorganic solution. UF membranes has a pore size of approximately 0.002 to 0.1 microns and is capable to remove particles with molecular weight in the range of 1,000 - 100,000 Dalton (Da) [22, 26]. UF operates by allowing water molecules and particles smaller than the pore size of the membrane to pass however, it retains particles larger than the pore size of the membrane [25]. Parameters such as pH, ligand concentration, applied pressure, and membrane pore size have been found to effect metal ion rejection rates [25]. Depending on the membrane characteristics, it has been reported that UF can achieve more than 90% removal efficiency of a metal concentration ranging from 10 - 112 mg/L at pH range of 5 - 9.5 and at pressure range of 2 - 5 bar. Drawbacks of this technique is low selectivity and frequent membrane fouling leading to high operational costs due to the need for constant membrane replacement, constant backwashing and chemical treatments [25].

2.6.4.2. *Nanofiltration (NF).* Nanofiltration has a separation mechanism which involves steric (sieving) and electrical (Donnan) effects. A Donnan potential is created between the charged anions in the NF membrane and the co-ions in the effluent to reject the latter [25]. The separation potential for NF membranes is in between UF

and RO. NF can achieve 90% removal efficiency of molecules with molecular weight range from 200 to 1,000 Da. NF generally has a nominal membrane pore size of approximately 0.001 microns [23, 26]. The significance of this membrane lies in its small pore and membrane surface charge. In general, NF membrane can treat inorganic effluent with a metal concentration of 2,000 mg/L. Depending on the membrane characteristics, NF can effectively remove metal at a wide pH range of 3 - 8 and at pressure range of 3 - 4 bar. However, NF is less intensively investigated than UF and RO for the removal of heavy metals [25].

2.6.4.3. ***Reverse osmosis (RO).*** RO is a pressure-driven membrane process where pressure is applied allowing water to pass through the membrane [26]. For this process to occur, the hydrostatic pressure which is applied should overcome the osmotic pressure of the wastewater solution. In comparison to UF and NF, RO is generally more effective for heavy metals removal and can achieve a removal efficiency of over 97% of a metal concentration ranging from 21 - 200 mg/L [25]. RO works effectively at a wide pH range of 3 - 11 and at pressure range of 4.5 - 15 bar. Since pressure is the driving force for this process, it is the major parameter that affects the extent of heavy metal removal, in which higher pressure will lead to higher removal efficiencies; thus, higher energy consumption [25]. RO is also characterized to be capable of handling high water flux rate, high salt rejection, resistant to biological attack, high mechanical strength, chemical stability, and the ability to withstand high operating temperatures. Drawbacks of this technique is similar to other membrane filtration types which are membrane fouling, high operational costs, high energy consumption, scaling of calcium carbonate $CaCO_3$ or calcium sulfate $CaSO_4$ and the requirement for experienced personnel to operate the process [25].

2.6.5. Electro dialysis (ED). ED is a process which uses a charged thin sheet of plastic membrane that can separate ionized species in the solution using an electric field as the driving force [25]. When a solution containing ionic species passes through the cell compartments, the anions migrate toward the anode and the cations toward the cathode, crossing the anion-exchange and cation-exchange membranes [25]. ED enables the recovery of valuable metals due to the concentrated stream produced. This process cannot effectively treat inorganic effluent with a metal concentration higher than 1,000 mg/L; thus it is more suitable for a metal concentration of less than

20 mg/L. Drawbacks of this process is that it requires relatively clean feed, careful operation and periodic maintenance to prevent any damages to the stack [25].

2.6.6. Membrane electrolysis (ME). ME is a chemical process driven by an electrolytic potential which is used to remove leftover heavy metals from already treated wastewater streams. There are two generally used cathodes: a conventional metal cathode or a high surface area metal cathode. The applied electrical potential across an ion exchange membrane forces reduction-oxidation reaction to take place on the electrodes. A study of the feasibility of electrochemical Cr(VI) removal from synthetic wastewater using carbon electrodes resulted in more than 98% removal efficiency with an initial chromium concentration of 8 mg/L at pH 2.0. ME offers wastewater treatment for a metal concentration of higher than 2,000 mg/L or less than 10 mg/L. A major disadvantage of using ME is its high-energy consumption [25].

2.6.7. Electrochemical precipitation (ECP). ECP process is similar to chemical precipitation but this process uses an electrical potential to increase its removal efficiency. Based on the characteristics of the electrodes, ECP can operate at acidic or basic conditions and can treat inorganic effluent with a metal concentration higher than 2,000 mg/L. This process can be carried out through electrochemical reduction-oxidation (redox) processes in an electrochemical cell without a continuous feeding of redox chemicals, thus avoiding a costly space, time, and energy consumption [25]. A study of the use of ECP for Cr(VI) removal from wastewater reported an efficiency of greater than 80% for an effluent with an initial Cr(VI) concentration of 0.5 mg/L [25].

2.6.8. Adsorption. Adsorption process is the buildup of substances at a surface interface through mass transfer [27, 28]. Mass transfer process occurs by diffusion of a liquid or a gas into a solid interface [27]. The diffusing component is the adsorbate and the material in which the adsorbate is diffusing to is the adsorbent [27]. Adsorption process is dependent on the adsorbent and adsorbate interaction and properties. This process can be used for a wide range of pH, operating temperatures and concentrations [29]. Adsorption can provide high efficiency with almost complete removal with relatively low energy consumption where the adsorbents can be easily regenerated and reused. Adsorption have been recognized for its capability to remove

various heavy metals from wastewater which was evaluated in several studies such as [30, 31, 32, 33, 34].

In this study, adsorption technique is selected for the removal of Cr(VI) from wastewater. This process has been selected due to its economical, simple, fast and efficient process characteristics in comparison to other discussed treatment techniques. Summary of the discussed techniques and their key features are shown in Table 2.5. In the following section, thorough review of adsorption theory, mechanism, equilibrium, kinetics and thermodynamics will be discussed.

Table 2.5: Summary of various techniques used to remove heavy metals from wastewater

Technique	Features	References
Chemical Precipitation	Simple and lost cost operation pH dependent Produced large volumes of low-density sludge	[22, 23]
Ion Exchange	High operating capacity and fast kinetics High removal efficiency pH and metal dependent Prone to fouling	[22, 23]
Coagulation and Flocculation	High operating capacity High operational cost High handling costs for toxic sludge disposal	[22, 24]
Membrane Filtration	High removal efficiency Require backwashing and chemical treatment Highly membrane dependent (membrane fouling) High operational and maintenance cost	[25, 26]
Electro Dialysis	Capable to recover valuable metals Requires clean feed and careful operation Requires periodic maintenance	[25]
Membrane Electrolysis	Treats already treated wastewater High energy consumption	[25]
Electrochemical Precipitation	Capable of handling high metal concentration Requires an energy source Large chemical consumption	[25]
Adsorption	Operates at wide pH Capable of treating low concentrations Does not require energy source to operate Can be easily regenerated and reused Dependent on adsorbate and adsorbent interaction	[27]

2.7. Overview of Adsorption

Adsorption was discovered by Lowitz, in 1785 and was subsequently used in sugar refining processes for color removal [27]. The term itself was coined by Kayser

in 1881 but has been reported as early as 4000 BC in Sanskrit texts as a method to enhance the taste and odor of drinking water [27]. Adsorption is generally used to recover specific component(s) or to remove an undesirable one(s) from an industrial effluent [23, 28]. Adsorption usually takes place in a bed packed with solid adsorbent. The fluid flows into the packed bed where mass transfer occurs at the adsorbent/adsorbate interface. When adsorbate is saturated, the bed is regenerated. The regeneration and desorption stage can be used to recover valuable metal(s) and/or reuse the adsorbent making the process relatively more cost effective. Adsorption process is divided into chemical adsorption and physical adsorption. Chemical adsorption is also known as chemisorption, this process involves activation energy and occurs when an adsorbate reacts with the adsorbent surface to form chemical bonds [27]. Moreover, physical adsorption is also known as physisorption, this process does not involve activation energy and occurs when an adsorbate undergoes physical attractive forces with the adsorbent surface without forming chemical bonds [27]. Physical adsorption is a reversible process due to the weaker bond forces and energies when compared to chemical adsorption. Naturally, physical forces operate over longer distances than chemical bonds and have no preferential surface adsorption sites [27]. For example, in water treatment, the adsorption of organic molecules onto activated carbon, is dictated by van der Waals forces [27].

Factors such as surface area, pore size and effluent matrix affect the efficiency of the adsorption process. Typically, as the pore size of an adsorbent decreases, the surface area increases which will reflect on the number and size of sites available for adsorption [27]. Additionally, depending on the size of the adsorbate and adsorbent pores, steric effects may limit the process of adsorption [27]. Lastly, effluents containing large amounts of natural and/or anthropogenic compounds are found to decrease adsorption capacity due to competitive adsorption on available sites [27]. The mechanism of adsorption takes place in three different steps shown in Figure 2.2 and are:

1. Film diffusion or external mass transfer (EMT)
2. Intraparticle diffusion or internal mass transfer (IMT)
3. Adsorption

Both film diffusion and intraparticle diffusion are based on diffusion processes and their driving force is based on the adsorbate concentration gradient between the bulk (C_b) and the internal surface (C_e) at equilibrium conditions. Film diffusion occurs through

the hydrodynamic layer around the adsorbent where it delivers the adsorbate to the external surface of the adsorbent. While intraparticle diffusion delivers the adsorbate to the adsorption site. Intraparticle diffusion occurs either through pore diffusion (D_p) or surface diffusion (D_s). Intraparticle diffusion is often the slowest step and thus it is the rate controlling step stating the overall uptake of an adsorbate. The final step is the actual adsorption which occurs quickly and is not considered a rate-limiting step [27].

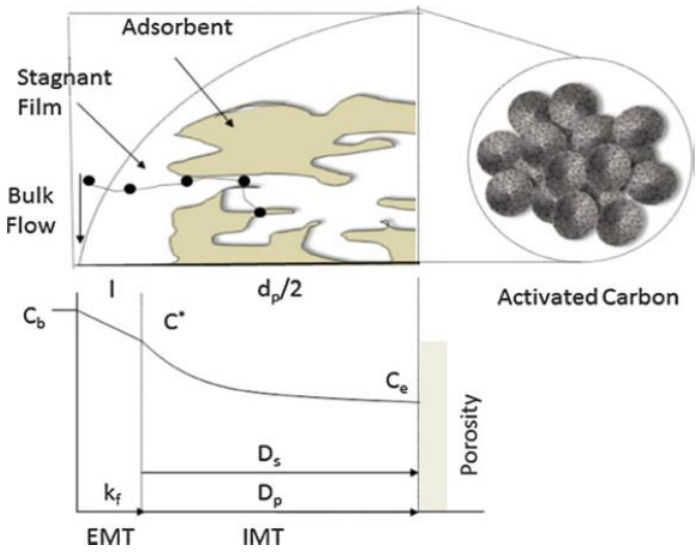

Figure 2.2: Schematic of mass transfer in adsorption process [27]

2.7.1. Adsorption equilibrium. Adsorption equilibrium is achieved when the adsorption rate is equal to the desorption rate. Equilibrium information is important to quantify the amount of adsorbate that an adsorbent can adsorb at equilibrium conditions and constant temperature [27]. Equilibrium conditions in a considered system depend on the interaction strength between the adsorbate and adsorbent, properties of the adsorbate and adsorbent, temperature, pH, and presence of any competing ions in solution [35]. The general form of equilibrium relationship for a single-solute is expressed as shown in Equation (1) [35]:

$$q_e = f(C_e, T) \tag{1}$$

where C_e and q_e are the adsorbate concentration and adsorbent loading at equilibrium and T is the temperature [35]. Equation (1) is commonly expressed at isothermal conditions where the equilibrium relationship can be expressed as given in Equation (2) [35]:

$$q_e = f(C_e) \tag{2}$$

For an experiment that varies the adsorbent dose and/or the initial adsorbate concentration, the equilibrium relation at constant temperature will provide the adsorption capacity of the given adsorbent at any adsorbate concentration. The equilibrium adsorption capacity is calculated using the mass balance expression given in Equation (3) [27]:

$$q_e = \frac{V}{M}(C_o - C_e) \tag{3}$$

where q_e is adsorbent loading at equilibrium (mg/g), C_o is initial concentration of adsorbate (mg/L), C_e is equilibrium concentration of adsorbate (mg/L), V is volume of aqueous solution added to bottle (L), and M is mass of adsorbent (g). Some adsorption equilibrium models that are commonly used in research include two parameters models which are Langmuir, Freundlich, Dubinin-Radushkevich (D-R), and Temkin. Three parameters equilibrium models include Sips isotherm, which is also described in this work [27].

2.7.1.1. ***Langmuir isotherm.*** Langmuir adsorption isotherm describes reversible chemical equilibrium between species at adsorbent and adsorbate interface [27]. This model assumes a constant value of free energy change for all surface sites and it also assumes that each site is capable of binding to only one molecule or, in other words, adsorption occurs up to a monolayer outer surface of the adsorbent [36]. Equation of Langmuir isotherm model to calculate adsorbent loading is expressed in Equation (4) [27]:

$$q_e = \frac{Q_m C_e K_L}{1 + C_e K_L} \tag{4}$$

where q_e is adsorbent loading at equilibrium (mg/g), C_e is equilibrium concentration of adsorbate (mg/L), Q_m is maximum monolayer adsorption capacity (mg/g), K_L is the Langmuir adsorption constant (L/mg). Equation (4) can be also written in a linear form as expressed in Equation (5):

$$\frac{C_e}{qe} = \frac{C_e}{Q_m} + \frac{1}{K_L Q_m} \tag{5}$$

where a slope of $\frac{C_e}{qe}$ versus C_e results in a straight line with $\frac{1}{K_L Q_m}$ as an intercept and $\frac{1}{Q_m}$ as a slope. Langmuir isotherm may be expressed in terms dimensionless parameter R_L, expressed in Equation (6), which specifies th adsorption nature. If R_L>1 adsorption is unfavorable, if R_L = 1 adsorption is linear and if R_L< 0 adsorption is favorable.

$$R_L = \frac{1}{1+(1+K_L C_o)} \quad (6)$$

2.7.1.2. ***Freundlich isotherm.*** Freundlich adsorption isotherm equation can be used to model data for heterogeneous adsorbents [27]. Freundlich isotherm cannot describe very low concentrations or very high concentrations but is often used to describe medium concentrations [35]. This isotherm is widely used for describing the adsorption from aqueous solutions onto activated carbon. It has become a standard equation for characterizing adsorption processes in water treatment for multi-solute systems [35]. Freundlich model equation is expressed in Equation (7) [27]:

$$q_e = K_f C_e^{\frac{1}{n}} \quad (7)$$

where q_e is adsorbent loading at equilibrium (mg/g), C_e is equilibrium concentration of adsorbate (mg/L), K_f is Freundlich adsorption capacity parameter ($mg^{1-1/n}.L^{1/n}$)/g), n is Freundlich adsorption intensity parameter. Equation (7) can be expressed in a linear form as shown in Equation (8):

$$log(q_e) = log(K_f) + \frac{1}{n} log(C_e) \quad (8)$$

where a slope of $\log(q_e)$ versus $\log(C_e)$ results in a straight line with $\log(K_f)$ as an intercept and $\frac{1}{n}$ as a slope. The parameter K_f characterizes the adsorption capacity, where higher values of K_f indicate larger adsorption capacity [35]. Whereas, exponent n relates to the energetic heterogeneity of the adsorbent surface and also the curvature of the isotherm. In principle, n can take any value however, in practice most n values are found to be lower than 1 which indicate normal adsorption [36]. When n = 1, the isotherm becomes linear which means adsorption is independent of the concentration [36]. When n < 1, the parameter indicates high adsorbent loadings at low concentrations. Therefore, isotherms with n < 1 are referred to as favorable, whereas isotherms with n > 1 are deemed as unfavorable.

2.7.1.3. ***Dubinin-radushkevich (D-R) isotherm.*** D-R isotherm model is used to describe adsorption data based on the theory of volume filling of micropores developed for vapor adsorption onto microporous adsorbents [35]. D-R isotherm is generally applied to express the adsorption mechanism with a Gaussian energy distribution onto a heterogeneous surface [36]. D-R isotherm expressed in Equation (9) [36]:

$$q_e = q_s \, exp(-K_{ad}\varepsilon^2) \quad (9)$$

where q_e is adsorbent loading at equilibrium (mg/g), q_s is the theoretical isotherm saturation capacity (mg/g), K_{ad} is D-R isotherm constant (mol^2/kJ^2) and ε is D-R isotherm constant expressed in Equation (10). This isotherm is usually applied to distinguish physical and chemical adsorption of metal ions with its mean free energy [36].

$$\varepsilon = RTln\left(1 + \frac{1}{Ce}\right) \tag{10}$$

where *R* is universal gas constant (8.314 J/mol.K), *T* is absolute temperature (K) and C_e is equilibrium concentration of adsorbate (mg/L). D-R isotherm model is temperature invariant and therefore, also referred to as the characteristic curve [35]. This model is often used for high solute activities and intermediate concentrations. Equation (9) is also expressed in a linear form as given in Equation (11):

$$ln(q_e) = ln(q_s) - K_{ad}\varepsilon^2 \tag{11}$$

where a slope of $ln(q_e)$ versus ε^2 results in a straight line with $ln(q_s)$ as an intercept and K_{ad} as a slope.

2.7.1.4. ***Temkin isotherm.*** Temkin isotherm model contains a factor that considers any interaction between the adsorbent and the adsorbate. This model ignores any low and large concentrations and assumes linearity of heat of adsorption of all molecules in the layer which would decrease linearly with surface coverage. The equation is derived using uniform distribution of binding energies and is expressed in Equation (12), where B in the Equation (12) is expressed in Equation (13):

$$q_e = B\,log(A_T) + B\,log(C_e) \tag{12}$$

$$B = \frac{RT}{b_T} \tag{13}$$

where *R* is universal gas constant (8.314J/mol.K), *T* is absolute temperature (K) and C_e is equilibrium concentration of adsorbate (mg/L), A_T is Temkin isotherm equilibrium binding constant (L/g), b_T is Temkin isotherm constant and *B* is a constant which relates to heat of sorption (J/mol) [36].

2.7.1.5. ***Sips isotherm.*** A three parameters isotherm model which is based on empirical isotherm defined as shown in Equation (14) [37]:

$$q_e = q_{th,m}^{e}\frac{K_e C_e^{n_s}}{1 + K_e C_e^{n_s}} \tag{14}$$

where q_e is adsorbent loading at equilibrium (mg/g), q_{th}^{e} is the theoretical maximum adsorption capacity (mg/g), n_s is sips constant, K_e is the equilibrium constant, C_e is equilibrium concentration of adsorbate (mol/L).

2.7.2. Adsorption kinetic models. Adsorption kinetic modeling is used to describe the rate of adsorbate uptake by the adsorbent and is one of the important characteristics which indicate residence time of an adsorption process. Many models have been developed in order to identify adsorption kinetics and the models described below include pseudo- first order, pseudo- second order and Elovich model [38, 39]:

2.7.2.1. ***Pseudo- first order***. Linear form of pseudo first order reaction model is expressed in Equation (15):

$$ln(q_e - q_t) = ln(q_e) - k_1 t \quad (15)$$

where q_e is adsorbent loading at equilibrium (mg/g), q_t is adsorbent loading at time t (mg/g), k_1 is the rate constant of pseudo- first order adsorption (min^{-1}) and t is time (min) [39].

2.7.2.2. ***Pseudo- second order.*** Pseudo- second order kinetic model is expressed in Equation (16):

$$\frac{t}{q_t} = \frac{1}{k_2 {q_e}^2} + \frac{t}{q_e} \quad (16)$$

where q_e is adsorbent loading at equilibrium (mg/g), q_t is adsorbent loading at time t (mg/g), k_2 is the rate constant of pseudo- second order adsorption (g/mg.min) and t is time (min) [39].

2.7.2.3. ***Elovich reaction model.*** Elovich reaction model is expressed in Equation (17):

$$q_t = \frac{1}{\beta} ln(\propto \beta) - \frac{1}{\beta} ln(t) \quad (17)$$

where q_t is adsorbent loading at time t (mg/g), $\propto$ and β represent the initial adsorption rate and desorption constant, respectively and t is time (min) [39].

2.7.3. Adsorption mechanism. Adsorption as described earlier occurs in three stages which are film diffusion, intraparticle diffusion and adsorption. However, since adsorption process is very rapid, it can be neglected from the kinetics study. Thus,

the kinetic process of adsorption is always controlled by film diffusion or intraparticle diffusion which are expressed in subsections below.

2.7.3.1. ***Film diffusion.*** Film diffusion is the transport of adsorbate from the bulk liquid to the external surface of the adsorbent particle where it can be expressed as shown in Equation (18) [35].

$$ln(1 - \frac{q_t}{q_e}) = -k_{fd}t + C \quad (18)$$

where q_e is adsorbent loading at equilibrium (mg/g), q_t is adsorbent loading at time t (mg/g), k_{fd} indicates the film diffusion rate constant (min^{-1}), t is time (min) and C provides information about the thickness of the boundary layer [35]. A plot of $ln(1 - \frac{q_e}{q_t})$ versus t will give a slope of k_{fd} and the intercept of C. If the plot of the experimental data for a given system is linear and passes through the origin, this means film diffusion is the rate determining step [39].

2.7.3.2. ***Intraparticle diffusion.*** Intraparticle diffusion, founded by Weber-Morris, is expressed in Equation (19) [39]:

$$q_t = k_{id}t^{1/2} + C_{id} \quad (19)$$

where q_t is adsorbent loading at time t (mg/g), k_{id} is intraparticle diffusion rate constant ($mg/g.min^{0.5}$) and C_{id} provides information about the thickness of the boundary layer. A plot of q_t and $t^{1/2}$ will give a slope of k_{id} and the intercept of C_{id}. If the plot of the experimental data for a given system is linear and passes through the origin, this means that intraparticle diffusion is the rate limiting step. However, if the plot does not pass through the origin, this means that there are other mechanisms contributing to the rate step which can be due to film diffusion. Moreover, large values of intercepts indicate higher contribution of surface adsorption in the rate limiting step [39].

2.7.4. Adsorption thermodynamics. Adsorption thermodynamic parameters are essential to fully understand an adsorption process. In thermodynamics, the state of a system is described by fundamental equations of thermodynamic potentials. The general precondition for a spontaneous reaction is that the change of free energy of reaction (ΔG) should have a negative sign. The equation which relates change of enthalpy (ΔH) and change of entropy (ΔS) to ΔG is the expressed in Equation (20) [35]:

$$\Delta G = \Delta H - T\Delta S \quad (20)$$

ΔS describes the change in the degree of disorder in a considered system and ΔH describes the heat of reaction [35]. Thermodynamic properties can be derived from Equation (21):

$$K_e = \frac{qe}{C_e} \tag{21}$$

where q_e is adsorbent loading at equilibrium (mg/g), K_e is the apparent equilibrium constant, C_e is equilibrium concentration of adsorbate (mg/L) [40]. ΔG, ΔH, and ΔS can be calculated from the Van't-Hoff equation [40].

$$\Delta G = -RTln(K_e) \tag{22}$$

where R is universal gas constant (8.314J/mol.K), T is absolute temperature (K), K_e is the apparent equilibrium constant. Substituting Equation (22) in Equation (20) will give Equation (23):

$$ln(K_e) = -\frac{\Delta H}{RT} + \frac{\Delta S}{R} \tag{23}$$

Substitution for K_e in Equation (21) into Equation (23) will give Equation (24):

$$ln(\frac{qe}{C_e}) = -\frac{\Delta H}{RT} + \frac{\Delta S}{R} \tag{24}$$

where a plot of $ln(\frac{qe}{C_e})$ versus $\frac{1}{T}$ will result with $-\frac{\Delta H}{R}$ as slope and $\frac{\Delta S}{R}$ as intercept.

2.8. Adsorbents

Adsorbents are the main component in an adsorption process, they are used to attach or collect adsorbates from a bulk gas or a bulk liquid phase onto their surface. Adsorbents used for wastewater treatment should be nontoxic, provide high adsorption capacity, adsorbs low concentrations of feed, such as in parts per billion (ppb), easily regenerated and are cost-effective [41]. Commonly used adsorbents in wastewater treatment are activated carbon, magnetic carbon, ferromagnetic carbon, alginate, sand, clay, chitosan, polyaniline, and ethyl cellulose, etc. Activated carbon has been proven to be an efficient and effective adsorbent for wastewater treatment since the 21st century for it can adsorb large organic molecules [27, 42]. It is famous for its high capacity and wide range of pore sizes, which are dependent on its manufacturing process [27, 42]. Manufacturing of activated carbon requires high heating temperatures of above 700 ^{o}C and pyrolysis in anaerobic environment. For wastewater treatment purposes, activated carbon is used in the form of granules or powder which are abbreviated as GAC and PAC, respectively. Other common adsorbents are zeolites and synthetic polymers [27].

Examples of adsorbents and their experimentally established adsorption capacities are summarized in Table 2.6 [28].

Table 2.6: Adsorption capacity of adsorbents for heavy metals in solution [28]

Adsorbent	Maximum adsorption capacity (mg/g)	Heavy metal	References
Fe_3O_4/activated carbon	71.42	Pb(II)	[43]
Mangrove/alginate	10.84	Pb(II)	[44]
ZSM-5 zeolite	20.1	Pb(II)	[45]
Pristine natural zeolite	14.93	Cu(II)	[46]
Polydopamine/natural zeolite	28.58	Cu(II)	[46]
Activated carbon (produced by chemical activation)	152.91	Cr(VI)	[47]
Activated carbon (produced by physical activation)	142.25	Cr(VI)	[47]
Crosslinked chitosan/bentonite	89.13	Cr(VI)	[48]
Magnetic carbon	278.8	Cr(VI)	[49]
Ethyl cellulose	12.2	Cr(VI)	[50]
Polyaniline-coated ethyl cellulose	38.76	Cr(VI)	[50]
L-lysine/crosslinked chitosan resin	70.34	Au(III)	[51]

In circumstances where the use of commercial adsorbents is deemed to be expensive and not feasible; the requirement to use non-conventional adsorbents was recognized. These adsorbents are characterized to be abundant in nature, inexpensive and require minimal processing [22]. Non-conventional adsorbents are also investigated due to the high thermal input required to manufacture conventional adsorbents [27]. A list of non-conventional adsorbents is given in Table 2.7 [27]. These adsorbents are utilized from agriculture waste, industry waste, natural materials, or natural substances which should have high surface area and porosity. Drawbacks of their use is that they are difficult to remove from the treated effluent [22].

Table 2.7: Examples of non-conventional adsorbents

Agriculture and industry waste	Natural materials	Bioadsorbents
• Teak wood bark • Seeds (papaya, etc.) • Sugar industry mud • Grass waste • Peels & shells (pomelo, jackfruit, etc.)	• Clay • Glass • Wool	• Biomass (algae, activated sludge.) • Fungi • Microbial

Recently, there is a great interest in the use of nanoparticles (NPs) as adsorbents due to their small pore size, large surface area, chemical activity and adsorption capacity [41]. Some of the used NPs adsorbents include carbon nanotubes (CNTs), manganese oxide, graphene, zinc oxide, magnesium oxide, titanium oxide and ferric oxides [41]. Classification of NPs adsorbents, given by International Union of Pure and Applied Chemistry (IUPAC), based on their pore size is the following [27]:

1. Macropores, pore sizes >25 nm
2. Mesopores, pore sizes between 1–25 nm
3. Micropores, pore sizes <1 nm

NPs CNTs have received a lot of attention since their discovery in 1991 due to their unique structure, physical and chemical properties [52, 53, 54]. In 2004, United States EPA expressed the need to explore environmental applications of CNTs, where remediation or treatment applications were chosen as one of the main areas of development [19]. Since then, CNTs have gained recognition for their adsorption capabilities due to their large specific surface area, as well as their small, hollow, and layered structures [55]. Various studies have shown the effectiveness of CNTs for the removal of metal ions [56, 57, 58, 59, 60].

In this study, MWCNTs are used as an adsorbent. MWCNTs are selected due to their large surface area and their hollow and layered structure which makes them fit for adsorption purposes. MWCNTs have multiple graphene layers which can be easily modified to increase their selectivity and efficiency. In comparison to single wall carbon nanotubes (SWCNTs), MWCNTs diameters can range from a few nanometers to dozens of nanometers. In addition, MWCNTs are commercially available at a relatively lower price than SWCNTs, making their use more feasible and practicable for industrial applications [61].

In the following sections, CNTs properties, synthesis, applications and functionalization will be discussed. In addition, few selected studies using MWCNTs for the removal heavy metals will be discussed.

2.8.1. Carbon nanotubes (CNTs). Carbon is a chemical element with atomic number six and has six electrons which occupy $1s^2$, $2s^2$, and $2p^2$ atomic orbitals. It can hybridize in sp, sp^2, or sp^3 forms [62]. The unique form of CNTs was first observed by physicist Sumio Iijima in 1991 [63]. CNTs are one of the most diverse and

rich NPs [52]. Advances in CNTs led to their use in rechargeable batteries, mobile screens, conductive additives, sporting goods and water filters [54]. CNTs offer a seamless structure with hexagonal honeycomb lattices, being several nanometers in diameter and many microns in length. CNTs are closed structures that present two well defined regions with different properties, the tube and the cap. Each end of the nanotubes is capped with half of a fullerene-like molecule that is responsible for the diameter of the tube. To obtain the convex structure, it is necessary to introduce a positive curvature into the planar hexagonal graphite lattice, this is accomplished by the introduction of topological defects [63, 64]. The unique structure of CNTs can be divided into two main types which are MWCNTs and SWCNTs [63]. A SWCNT consists of one atomic layer thick sheet with graphene sheet rolled into a perfect cylinder however, MWCNTs are built of a set of graphene cylinders which can be considered as several individual SWCNTs with increasing diameter and are placed concentrically inside each other. SWCNTs have three structures: armchair, zigzag, and chiral and they typically have a diameter value of around 1 nm, while MWCNTs have diameters of a few tens of nanometers [64]. Figure 2.3a and Figure 2.3b shows the structure of SWCNTs and MWCNTs, respectively [64].

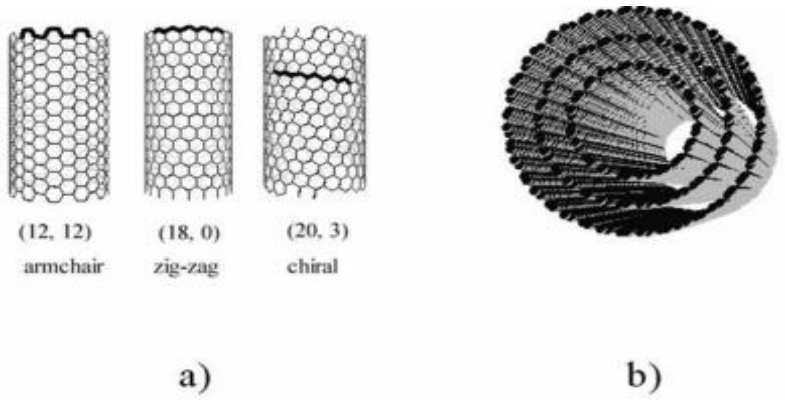

Figure 2.3: Structures of a) SWCNTs and b) MWCNTs [64]

2.8.2. CNTs synthesis. There are definitely some challenges in the production process of CNTs. Few of these challenges include, bulk production of high-quality products, low product selectivity, difficulty to control and predict structure and electronic properties of products, organization, orientation of the product on a flat substrate, and the development of a thorough understanding of the growth processes. Recent advances in production and purification techniques permitted the accessibility of good-quality CNTs in large quantities where production volumes of MWCNTs have

exceeded a few hundred tons per year however, SWCNTs production has not yet exceeded a few kilos [54, 65]. The following subsections will focus on the main techniques used to for the synthesis of CNTs.

2.8.2.1. ***Electric arc-discharge.*** Electric arc-discharge is the first method used to synthesize CNTs. In 1992, a breakthrough in MWCNTs growth was achieved by Ebbesen and Ajayan whom were able to achieve growth and purification of high-quality MWCNTs at gram level. In 1993, first success in producing substantial amounts of SWCNTs was achieved by Bethune and his coworkers [66]. This process consists of an electric arc discharged between two graphite electrodes separated by inert helium gas. Stable discharge plasma used is achieved using rotating electrode process which distributes micro discharges between the electrodes or using liquid nitrogen between the electrodes to provide an inert and temperature-controlled environment [52]. At elevated temperatures, the anode gets sublimated and deposited on the cathode and its surrounding wall. Parameters such as gas type, pressure, flowrate, electric field strength, electrode materials and dimensions, along with the apparatus size and geometry control CNTs production using this process [52].

2.8.2.2. ***Laser ablation.*** The first CNTs synthesis using this technique was reported in 1995. This process provides a better control over the growth of CNTs than electric arc-discharge technique [67]. High quality SWCNTs of 1-10 g scale was achieved by Smalley and coworkers [66]. This process consists of a solid graphite mounted in a quartz tube and placed in a temperature-controlled oven. Neodymium-Doped Yttrium-Aluminum-Garnet (Nd:YAG) laser is pulsed on the graphite in order to vaporize it. Carbon based powder is then collected from the inside of the apparatus. Introduction of an additional Nd:YAG delayed slightly behind the first pulse can improve the system. Also, the addition of equal amount of (0.5 - 1.0 atom %) of cobalt and nickel powders in graphite have been found to aid in the efficiency of SWCNTs production [52].

2.8.2.3. ***Chemical vapor deposition (CVD).*** This process is the most used and accepted technique for CNTs production, due to its simple and low temperature operation, bulk production and relatively low cost [67]. Basically, this process consists of gas molecules with high carbon content pyrolyzed at high temperatures with the presence of catalyst. This process can be done by a supported growth which uses a

catalyst prepared and placed on flow apparatus where it is exposed to elevated temperatures in the range of 500 - 1100^{o}C at a given time or by a process called floating-catalyst growth where the catalyst and carbon source are injected simultaneously. The reaction can then take place in the gas flow or following self-deposition on the surface of the reactor [52, 65]. This process allows for CNT diameter selectivity by controlling the catalyst deposition. Floating catalyst methods contribute to the production of SWCNTs, while most of other CVD-based methods produced mainly MWCNTs [52, 64].

2.8.2.4. ***Hydrothermal.*** This technique takes place in a closed system using heterogeneous reaction with the presence of aqueous solvents or metallic material, under pressure and temperature capable of dissolving and recrystallizing the insoluble material. The most important parameters in this process are temperature and pressure for they directly affect the dissolution process. CNTs produced using this method do not require a catalyst metal at elevated temperatures. This process produces MWCNTs with diameter of around 10 nm and length of hundreds of nanometers. This procedure has not been reported for SWCNTs preparation or commercial production of CNTs. This technique is environmentally friendly due to the absence of hazardous elements in the reaction, moderate pressure and temperature operation, low energy consumption and high yield [67]. From all of the above techniques used for CNTs synthesis, CVD method appears to be the best process for large quantities of MWCNTs. However, CNTs production with elevated purity, uniform size, large scale and low cost remains the biggest concern in the academic community. Table 2.8 summarizes the discussed synthesis techniques along with their products, advantages and disadvantages [67].

2.8.3. CNTs properties and applications. CNTs structure, geometric properties and dimensions have characterized their unparallel physical properties. These properties comprise of mechanical properties, thermal stability and enormous thermal and electrical conductivity [65]. Their properties are dependent on the type of CNTs, diameter, length, and chirality of the material [67]. CNTs are known for their ultra-high mechanical strength quantified by Young's modulus being around 1 TPa and tensile strength between 11 – 63 GPa [68]. At low temperatures, CNTs are brittle regardless of their diameter or helicity however, at room temperature they are flexible due to their high strength and capability to distort in order to release stresses [69]. CNT

are also metastable, where a hierarchy of thermal stabilities arranged by increasing order is the following: graphite > MWCNTs > SWCNTs > fullerenes. Furthermore, their thermal conductivity surpasses diamond at a value of 2,000 W/m.K [65]. Moreover, current research in CNTs is focused to explore their interesting heat transport properties [65]. The physical properties of CNTs are made to use through their wide applications in areas such as electronics, energy, composites, sensors, field emission, biology and other miscellaneous fields [65]. In area of electronic, metallic and semiconducting applications, SWCNTs are found to possess electrical characteristics that compare favorably with the best electronic materials. Recent advances in SWCNTs have enabled the development of field-effect transistors (FET). The metallic characteristics of CNTs allowed them to function as interconnects. It has been reported that CNTs can withstand current densities up to 1,010 A/cm^2 which exceed the value of copper by a factor of one thousand [65]. In the area of energy generation and storage applications, CNTs show a great potential for the use as super capacitors, lithium-ion batteries, solar cells and fuel cells. A large amount of research is focused on the application of CNTs in lithium-ion batteries due to their high reversible capacity reaching up to 1,000 mAh/g [65]. CNTs are considered to be the ideal form of fibers with superior mechanical properties compared to the best carbon fibers. Carbon fibers have been used as reinforcements typically found in expensive tennis rackets, space crafts and aircraft body parts. However, properties of CNTs have driven key organizations such as NASA, to invest in their development for aerospace application [65]. There is a potential for the use of SWCNTs as gas detector sensors due to their electronic structure being better than conventional metal oxide based sensors. They have better properties in terms of energy consumption, sensitivity, and size. CNTs are also promising electrodes in electrochemical sensors due to their fast electron transfer kinetics [65, 67]. In biomedicine applications, CNTs have been proven to be capable of increasing electrochemical reactivity of important biomolecules and promote direct electron transfer reaction of proteins. Thy can also be used as biosensors where they can detect molecules such as DNA, ATP, oxygen (O_2), nitrogen (N_2) hydrogen peroxide (H_2O_2), nitrogen oxide (NO), protein, biomarker and glucose. Lastly, CNTs are currently studied in nanodrug delivery applications for they can easily enter cell membranes and exhibit blood circulation half-lives in a factor of hours [67].

Table 2.8: CNT synthesis methods, products, advantages and disadvantages [67]

Method	Product	Advantage	Disadvantage
Electric arc-discharge	• SWCNT ϕ:0.6–1.4 nm • MWCNT ϕ:1–3 nm Medium purity	Few defects, no catalyst, not too expensive, open air	Carbon impurities, other nanoparticles, short CNTs
Laser ablation	• SWCNT ϕ:1–2 nm • MWCNT ϕ:1–3 nm Low purity	Good quality, highest yield, narrower distribution of SWCNT diameter	Very high-cost, impure CNTs
CVD	• SWCNT ϕ: 0.6–4 nm • MWCNT ϕ:10–240 nm Medium to high purity	Scalable up to industrial production, diameter controllable	SWCNT and MWCNT mixture
Hydrothermal	• MWCNT ϕ:5–8 nm Low purity	Easy process, low temperature	Low-scale production, many defects, difficult controls

2.8.4. CNTs functionalization. As discussed earlier, different CNTs have different properties however, it is very common that CNTs aggregate and form bundles, which adversely affects their properties and their solubility in aqueous and non-aqueous solutions. The insoluble properties of CNTs are owed to their high van der Waals attractions. Over the years, a wide range of techniques was used to improve its solubility, dispersibility and surface interaction. Chemical functionalization is used to enhance their solubility, improve their interactions, and change the behavior of some polymers and by that, this process allows their use in several applications. CNT bundles can be generally broken by ultrasonication followed by chemical reagent modification which aids in changing CNT surface and prevents their reaggregation [67]. The common methods for chemical functionalization are covalent and non-covalent functionalization. Covalent functionalization is based on the formation of covalent chemical bonds between CNT walls and a chemical reagent while non-covalent functionalization is related to the intermolecular interactions between CNT walls and a chemical reagent by van der Waals forces. CNTs can be covalently functionalized with different chemical groups, such as carboxylic (–COOH), alkyl ($–C_6H_{11}$), amide and phenyl groups. Many approaches have been developed for CNT covalent functionalization, but the challenge is to find the best method to improve a specific

property of interest, whether it is mechanical, electrical, optical, etc. Nowadays, non-covalent functionalization of CNTs has been more commonly used. This technique is characterized to introduce fewer defects in the graphitic structure which enhances solubilization and maximizes intrinsic characteristics of an individual CNT without changing its original structure or electronic properties. Low molecular weight surfactants, amphiphilic polymers, or even some organic molecules are commonly used as non-covalent functionalization reagents. Other functionalization techniques have been also developed to optimize the already existing ones and these include, click chemistry functionalization, used for biosensing applications, and defect functionalization, obtained by an oxidation process. The new developments in the processes for functionalization have widened the opportunities for CNTs applications in various fields [67].

2.8.5. Studies of CNTs for removal of heavy metals from wastewater.

Research around the application of CNTs in adsorption is vast and is widely diverted towards wastewater remediation techniques. The increased recognition is linked to the fact that they can be easily modified to increase its selectivity and removal efficiency. This subsection summarizes few of the findings and examples of research completed using MWCNTs for various wastewater applications.

- Research on the removal of antimony from an aqueous solution by raw MWCNTs was investigated. The results revealed that 80% of the antimony was removed from the aqueous solution within 30 min, at pH 7.0, using 200 mg MWCNTs, at 298 K [70].
- Removal of aniline from an aqueous solution by MWCNTs was studied using two ranges of MWCNTs diameters, 10 - 20 nm and 40 – 60 nm. The removal was obtained to be 94% for MWCNTs with diameter 10 - 20 nm and 92% for MWCNTs with diameter 40 - 60 nm at 40 mg dosage in 20 mL solution, pH of 7, temperature of 298 K, and aniline initial concentration of 50 mg/L [71].
- The adsorption of 2,3-dichlorophenol, an organic pollutant, by MWCNTs in aqueous solution revealed that 94% of the pollutant was removed by MWCNTs dosage of 200 mg [72].
- The adsorption of various coexisting metals was studied using MWCNTs modified with iminodiacetic acid (IDA). Results revealed that the adsorption capacity of Cr(VI) coexisting with other heavy metals was 8.96 mg/g. A study on the effect of

pH showed that adsorption is best at pH of 8 for all the coexisting metals in solution [73].

- The adsorption using nitric acid oxidized MWCNTs (ox-CNx) to remove cadmium and lead in aqueous solution was studied. The results revealed that adsorption of lead was higher than cadmium when both metals are in solution at pH of 5 and temperature of 25 ^{o}C. Adsorption capacities for cadmium and lead were reported to be 0.083 and 0.139 mmol/g, respectively [74].
- The adsorption of cadmium was also studied for three CNTs modifications which were oxidized nitrogen-doped MWCNTs (ox-N-MWCNTs), oxidized MWCNTs (ox-MWCNTs), and oxidized SWCNTs (ox-SWCNTs). Cadmium adsorption isotherms were determined at pH 6. Results revealed that ox-SWCNTs cadmium adsorption capacity is about three and six times higher than for ox-N-MWCNTs and ox-MWCNTs, respectively [75].

Research on the application of MWCNTs for the removal of Cr(VI) were also reviewed and few are summarized as follows:

- Magnetic MWCNTs were used as adsorbents for the removal of Cr(VI) in aqueous solutions. Results revealed that adsorption is pH dependent and best removal was achieved at pH of 3. Adsorption kinetics were best represented by the pseudo second- order kinetic model, and the adsorption isotherms were best fitted to Langmuir model with adsorption capacity of 12.531 mg/g at 20 ^{o}C. Calculation of Gibbs free energy and enthalpy of reaction revealed that the adsorption process was a spontaneous and endothermic reaction. The magnetic MWCNTs showed significant potential for application in adsorption of heavy metal ions [76].
- The adsorption of Cr(VI) ion was also studied using unmodified SWCNTs and MWCNTs and it was observed that the removal efficiency of Cr(VI) ions is highly dependent on pH of solution where a maximum efficiency was achieved at pH 2.5. Langmuir model best fitted the obtained results providing maximum adsorption capacities of Cr(VI) ions by MWCNTs and SWCNTs of 1.26 and 2.35 mg/g, respectively. Kinetic studies were found to be best fitted to pseudo- second order model [24].
- The adsorption of Cr(VI) at very low concentrations was studied using three adsorbents which were activated carbon, functionalized MWCNTs (f-MWCNTs) and unfunctionalized MWCNTs (unf-MWCNTs). The results revealed that the unf-

MWCNTs provided the highest adsorption efficiency of 98% at an initial Cr(VI) concentration of 100 ppb. The results also showed that f-MWCNTs and unf-MWCNTs were better adsorbents when compared to activated carbon [19].

- In a study which investigated the adsorption of Cr(VI) using MWCNTs in aqueous solutions, it revealed that adsorption isotherms were best fitted to Langmuir isotherm model with an adsorption capacity of 27.8 mg/g at 300 K. The best removal was achieved at a pH range of 1 - 2. The kinetic data fitted well with the pseudo- second order kinetic model. Thermodynamic parameters revealed a spontaneous, physical and endothermic adsorption [37].
- In a study which synthesized and used manganese dioxide/iron oxide/acid oxidized MWCNTs magnetic composites (MnO_2/Fe_3O_4/o-MWCNTs) as adsorbents for Cr(VI) adsorption revealed that pH has a direct effect on adsorption capacity, in which highest removal was achieved at pH of 2. Adsorption isotherm was fitted to Langmuir isotherm model with adsorption capacity of 186.9 mg/g at 335 K. The kinetic data fitted well with the pseudo- second order kinetic model [77].
- The adsorption of Cr(VI) at very low concentrations was also studied by using four different adsorbents which were powdered activated carbon, chitosan, SWCNTs, and MWCNTs. Highest adsorption of Cr(VI) was achieved at pH of 4, and adsorbent dosage of 100 mg/L. Powdered activated carbon and chitosan provided the best removal efficiencies of 99.4% and 94.7%, respectively; while the removal efficiencies of SWCNTs and MWCNTs were 72.9% and 51.9%, respectively. Adsorption isotherms were well-fitted to Langmuir isotherm model and the adsorption capacities for Cr(VI) were found to be 46.9, 35.6, 20.3, and 2.48 mg/g for PAC, chitosan, SWCNTs, and MWCNTs, respectively. The kinetic data fitted well with the pseudo- second order kinetic model [78].

Chapter 3. Materials and Methods

3.1. Materials

MWCNTs (>95%) were obtained from Grafen Chemical Industries Co (KNT-M31, Turkey) with less than 8 nm diameter and 10-30 µm length. All chemicals used in the experiments were of analytical grade unless specified otherwise. Double distilled water was used in all experiment. Potassium dichromate ($K_2Cr_2O_7$) was obtained from S-D Fine-Chem Limited (India). Cetyl trimethylammonium bromide (CTAB) was obtained from Fisher Scientic (U.K.). 1.0 M hydrochloric acid (HCl) and 1.0 M sodium hydroxide (NaOH) were used for pH adjustments. Finally, 0.1 M potassium chloride (KCl) was used as regeneration reagent.

3.2. Instrumentation

Double distilled water was generated using Water Still Aquatron A4000D, UK. Samples were shaken in a temperature-controlled flask shaker (Edmund Buhler, Germany). Syringe filters of 0.22 and 0.45 µm purchased from MCE Membrane, membrane solutions (USA) were used to filter the MWCNTs-CTAB from the aqueous solution. A pH meter by Orion 201A+, Thermo Electron Corp., USA was used for pH measurements and adjustments. Hot box oven with fan (GALLENKAMP, UK) set at 105 ^oC was used for drying. A Cary 50 spectrophotometer (Varian, Australia) at 540 nm was used for Ultraviolet-Visible spectrophotometer (UV–VIS) Cr(VI) measurements. Characterization of MWCNTs samples was performed using Fourier Transform Infrared (FTIR) spectra (PerkinElmer, U.S.A.), a wavelength range of 4000 – 400 cm^{-1} was used to study the surface chemistry. Thermogravimetric Analyzer (TGA) (PerkinElmer, USA) was used to investigate the thermal stability of the samples. The samples were heated from 30 ^oC to 800 ^oC at a heating rate of 10 ^oC/min, in nitrogen (N_2) atmosphere with a flow rate of 20 mL/min. Energy Dispersive X-ray Spectroscopy (EDS) (Oxford instruments, UK) and Scanning electron microscopy (SEM) were used to investigate the elemental components and surface morphology of the samples. SEM was done using Tescan VEGA XMU, LaB6 filament, Oxford Instruments X-Max 50 SSD detector. Surface area analysis were carried out using nitrogen adsorption–desorption isotherms at 77 K using Quantachrome gas sorption analyzer (Autosorb iQ, USA).

3.3. Methods

3.3.1. Adsorption experiment. The effect of adsorbent dosage, contact time, pH, temperature and initial metal concentration on the removal efficiency of Cr(VI) were studied using batch adsorption experiments. The effect of each parameter was studied by varying it while keeping other parameters constant. The removal efficiency percentages were calculated using Equation (25):

$$Removal\ \% = \frac{C_o - C_e}{C_o} * 100 \quad (25)$$

where C_o and C_e are the initial concentration and equilibrium concentration (parts per millions, ppm), respectively. To conduct the adsorption experiments, 500 ppm stock solution of Cr(VI) was prepared and further diluted by double distilled water to the required concentration for each experimental study. The pH of the samples was adjusted using 1.0 M HCl and 1.0 M NaOH. 10 mL of Cr(VI) solution was introduced to 50 mL erlenmeyer flask where a measured known mass of the adsorbent was added. The 50 mL flasks were then placed in temperature-controlled shaker at rate of 150 rpm. After a specific time interval, the samples were filtered using 0.22 or 0.45 µm syringe filters and analyzed. Final Cr(VI) concentration was measured at 540 nm using UV–VIS by 1,5 diphenylcarbazine method [79]. For each experiment, two runs along with a blank control sample were carried out. All the glassware used in the experiments were washed thoroughly with double distiller water before drying in the hot box oven.

3.3.2. Quality assurance method. For control and reproducibility purposes, an experimental study was conducted which verified whether free CTAB, which is CTAB unattached to MWCNTs in solution, were responsible for removal of Cr(VI). The study consisted of two separate 50 mL erylernmeyer flasks. One flask contained 0.1 mM CTAB solution mixed with 100 ppm Cr(VI) solution and other flask contained an identical solution with an addition of 0.05 g of raw MWCNTs. The two 50 mL flask samples were placed in a temperature-controlled shaker at speed of 150 rpm for a contact time of 30 min at a temperature set at 25 ^{o}C. The samples were then filtered and analyzed. The final amount of Cr(VI) in solution was obtained using the method described in subsection 3.3.1 and results obtained are discussed in the Chapter 4.

3.3.3. Surface modification. To modify MWCNTs surface with CTAB, 0.5 g of raw MWCNTs were added to 500 mL of 10 mM CTAB aqueous solution. Well dispersed MWCNTs-CTAB complex was obtained by stirring the mixture at stirring speed of 240 rpm for 24 hours and then stirring speed was decreased to 80 rpm and the samples were kept for an additional 24 hours. Then, the dispersed MWCNTs-CTAB complex were vacuum filtered. The filtrate was then washed with an optimum amount of double distilled water. The process of obtaining the optimum amount of double distilled water consisted of an adsorption study on the effect of double distilled water volume on removal efficiency of the produced modified samples. Adsorption study involved three volumes of double distilled water; severe and rigorous washing of filtrate with volumes between 300-400 mL, a relatively less severely washed filtrate with volume of approximately equal to 250 mL, least washing with volume approximately equal to 100 mL. The results of all the three concluded that washing the filtrate with 100 mL of double distilled water provided the modified sample with highest capabilities to adsorb Cr(VI); therefore, 100mL washing volume was used as the optimum amount to modify all the used samples. After washing, the filtrate was dried at 105℃ in hot box oven for 24 hours.

3.3.4. Regeneration. For regeneration and reusability purposes, MWCNTs-CTAB regeneration study was carried out. Adsorption experiment studies were conducted at optimum conditions and then the samples were collected, dried, and regenerated using 0.1 M KCl aqueous solution. In a 100 mL erylernmeyer flask 0.5 g of Cr(VI)-saturated MWCNTs-CTAB was added to the regenerating solution. The flasks were then shaken at speed of 150 rpm for contact time of 30 min in temperature-controlled shakers at two different temperatures which were 25 ^{o}C and 35 ^{o}C separately. After desorption, the adsorbents were filtered and dried at 105 ^{o}C in hot box oven for 24 hours and used for adsorption at optimum conditions established in this study. These samples were then used for another regeneration-adsorption cycle. The final amount of Cr(VI) in each adsorption cycle was obtained using the method described in subsection 3.3.1.

Chapter 4. Results and Discussion

4.1. Surface Characterization

Surface characterizations of both raw and modified MWCNTs were performed using TGA, FTIR, BET, SEM and EDS. Results of each method will be discussed in the following subsections.

4.1.1. TGA. The TGA obtained for CTAB, raw MWCNTs and MWCNTs-CTAB complex are shown in Figure 4.1. The results obtained show that MWCNTs is a fairly stable compound with no volatile compounds, this is evident from the negligible weight loss seen as the temperature increase. Results for CTAB show that at a temperature range of 200 ^{o}C – 300 ^{o}C, the compound was fully degraded which agrees with literature where CTAB's decomposition temperature is at T > 235 ^{o}C [80]. TGA results of the modified MWCNTs-CTAB confirm that CTAB was attached to raw MWCNTs, this is evident by the degradation seen at a similar temperature range as the CTAB sample.

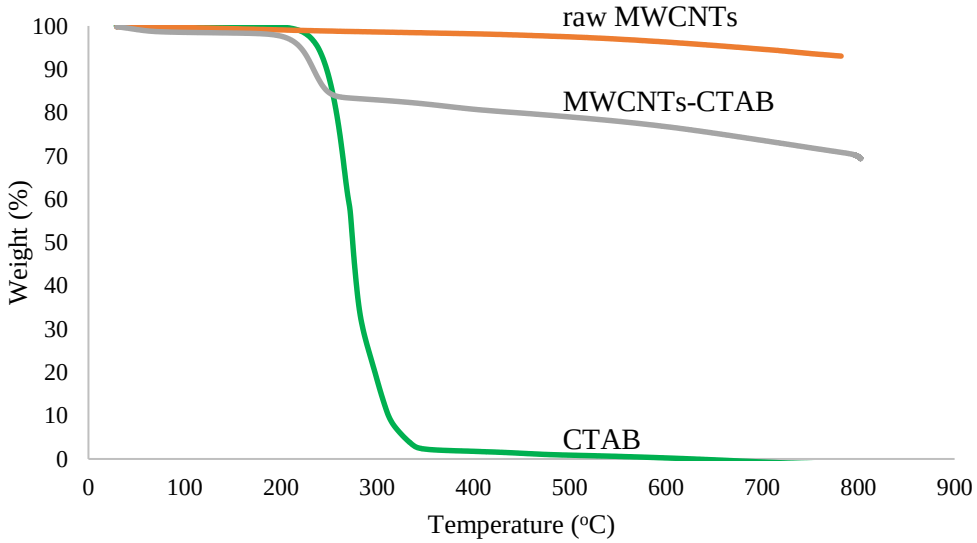

Figure 4.1: TGA results showing weight loss (%) versus temperature (^{o}C) for CTAB, raw MWCNTs, modified MWCNTs with CTAB.

4.1.2. FTIR. The FTIR spectrum of CTAB, raw MWCNTs and newly modified MWCNTs-CTAB are shown in Figure 4.2a. Peaks common for all the samples were identified at 3440 cm^{-1} and 1050 cm^{-1} and are assigned to O-H stretching and C-O stretching, respectively. In addition, peaks at 2920 cm^{-1} and 2850 cm^{-1} attributed to asymmetric C-H stretching and symmetric C-H stretching, respectively

[81]. For raw CTAB, bands at 1630 cm^{-1} and 1468 cm^{-1} belong to asymmetric and symmetric stretching vibration of N+-CH_3; similar peaks were obtained at 1630 cm^{-1} and 1406 cm^{-1} for MWCNTs-CTAB sample [81]. FTIR was also completed on MWCNTs-CTAB sample after adsorption of Cr(VI). The results obtained are shown in Figure 4.2b along with the FTIR result of the newly modified MWCNTs-CTAB (prior to adsorption). The FTIR revealed that the peaks at 1406 cm^{-1} and 1050 cm^{-1} seem to have disappeared. The peaks at 2920 cm^{-1} and 2850 cm^{-1} have widen and lost their intensity. The disappearance of the bands and the change in their intensity could be due to surface modification of the samples and probable binding to Cr(VI). This observation can suggest that these bonds played a major role in the adsorption of Cr(VI) [82]. Similar results were seen in a study of raw graphene and graphene modified with CTAB before and after adsorption of two types of dyes [83]. Lastly, FTIR was also done on the regenerated samples at 25 ^{o}C and 35 ^{o}C. The identified peaks are summarized in Table 4.1. The intensity of the peaks before and after adsorption decreased as seen in the adsorbed MWCNTs-CTAB sample in Figure 4.2b. It is important to note that for the second regeneration-adsorption cycle, the peaks were even less intense in comparison to the peaks present at the first regeneration-adsorption cycle. Since the FTIR peaks and intensity were not retained after regeneration this suggests that Cr(VI) ions were still attached to the functional groups and were not fully released into the regenerating solution during regeneration.

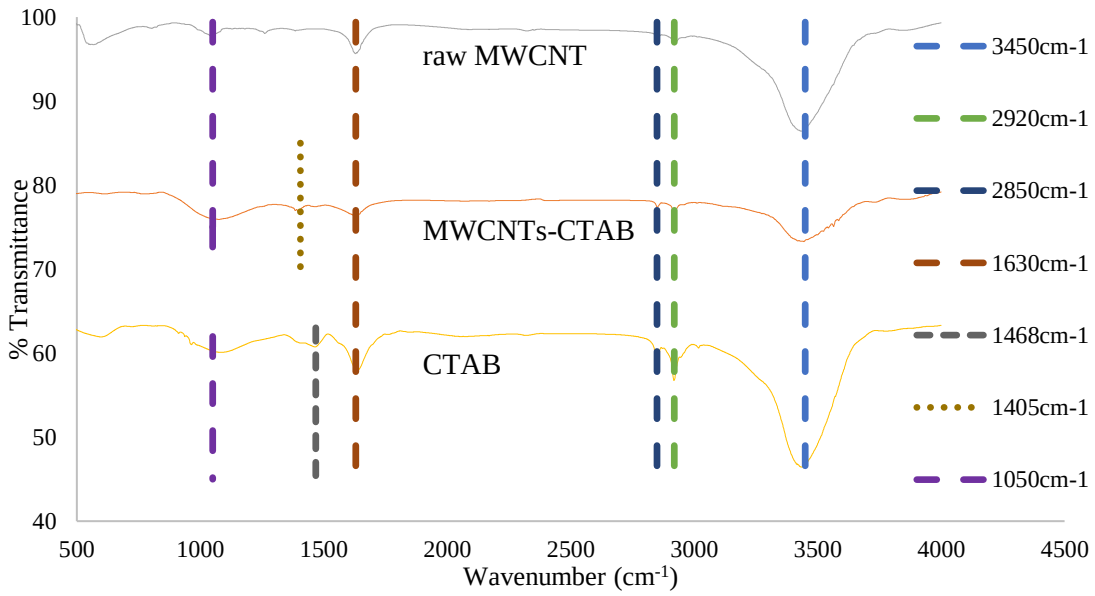

Figure 4.2a: FTIR results of raw MWCNTs (top), MWCNTs-CTAB (middle), CTAB (bottom)

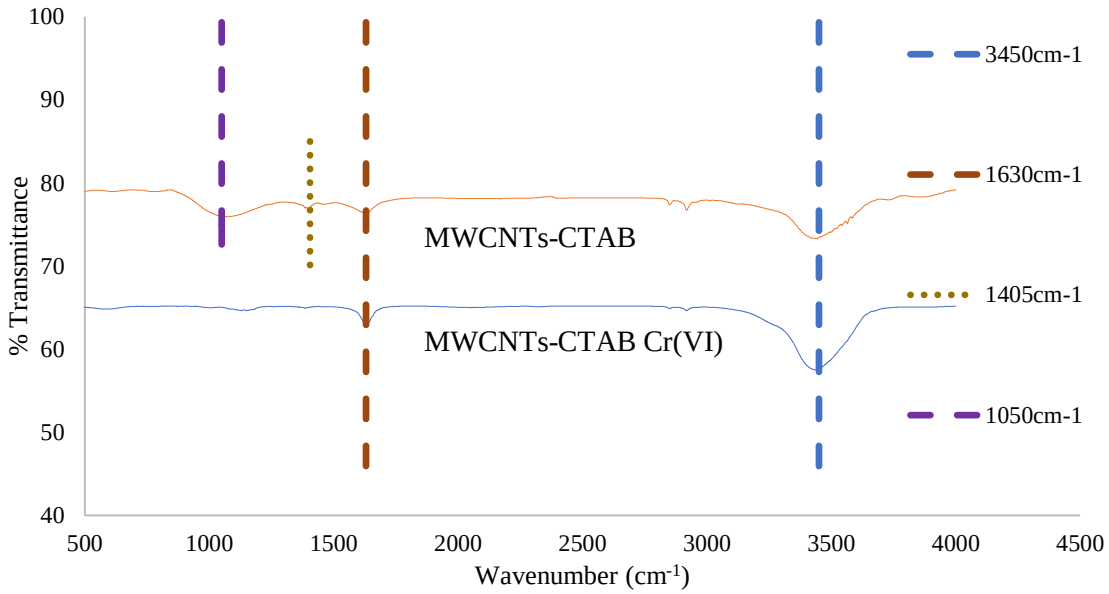

Figure 4.2b: FTIR result of MWCNTs-CTAB (top) before adsorption of Cr(VI) and FTIR result of MWCNTs-CTAB Cr(VI) (bottom) after Cr(VI) adsorption

Table 4.1: Summary of FTIR peaks of the regenerated samples

Functional band peaks (cm^{-1})	Regenerated sample 1, 25 ^oC, before adsorption	Regenerated sample 1, 25 ^oC, after adsorption	Regenerated sample 2, 25 ^oC, before adsorption	Regenerated sample 2, 25 ^oC, after adsorption
3450	✓	✓	✓	✓
2920	✓	✓	✓	✓*
2850	✓	✓	✓*	✓*
1630	✓	✓	✓*	✓
1405	✗	✗	✗	✗
1050	✗	✗	✗	✗
Functional band peaks (cm^{-1})	Regenerated sample 1, 35 ^oC, before adsorption	Regenerated sample 1, 35 ^oC, after adsorption	Regenerated sample 2, 35 ^oC, before adsorption	Regenerated sample 2, 35 ^oC, after adsorption
3450	✓	✓	✓	✓
2920	✓	✓	✓*	✓*
2850	✓	✓	✓*	✓*
1630	✓	✓	✓	✓
1405	✗	✗	✗	✗
1050	✗	✗	✗	✗

* Peaks with very low intensity

4.1.3. Surface area analysis. The surface area analysis results for raw MWCNTs and MWCNTs-CTAB are given in Table 4.2. The surface area for

MWCNTs slightly decreased with the modification of CTAB meaning CTAB did not increase the surface area/porosity of MWCNTs but changed its characteristics and surface charge to easily bind to Cr(VI) ions in the solution.

Table 4.2: Surface area results for raw MWCNTs and MWCNTs-CTAB

Sample Name	Surface area (m^2/g)
Raw MWCNTs	191.022
MWCNTs-CTAB	164.765

4.1.4. SEM. SEM results of raw MWCNTs, MWCNTs-CTAB, MWCNTs-CTAB after adsorption and regenerated MWCNTs-CTAB samples are shown in Figure 4.3(a), (b), (c) and (d), respectively. From SEM result for (b), representing MWCNTs-CTAB, it is evident that the pores and voids were modified as compared to SEM results (a), representing raw MWCNTs. SEM image (c) representing MWCNTs-CTAB after adsorption of chromium ions shows that the surface was occupied and filled when it is compared to the unadsorbed samples, SEM image (b). Whereas, the regenerated sample, SEM image (d), shows that the surface is still filled and did not retain back its surface characteristics prior to adsorption (shown in SEM (b)) and thus, this can have an impact on its regeneration efficiency.

4.1.5. EDS. EDS analysis of raw MWCNTs, MWCNTs-CTAB and MWCNTs-CTAB after adsorption of Cr(VI) are shown in Figure 4.4(a), (b) and (c) respectively. Results for MWCNTs, Figure 4.4(a), express a carbon content of 94.3% and absence of chromium. After modification of MWCNTs with CTAB, Figure 4.4(b), the carbon content decreased to 90.1% and no presence of chromium was evident. Lastly, Figure 4.4(c) which represent the adsorbed MWCNTs-CTAB samples confirms the presence of chromium and therefore verifying that adsorption of chromium was successful.

4.2. Quality Assurance Results

The study of 0.1 mM CTAB in 100 ppm Cr(VI) solution showed a low 3% removal of Cr(VI), while the results obtained for the same solution dispersed in 0.05 g MWCNTs showed 11% removal of Cr(VI). This study can provide confidence in the adsorption results by assuring that CTAB free in solution and unattached to MWCNTs cannot significantly affect the removal efficiency of Cr(VI).

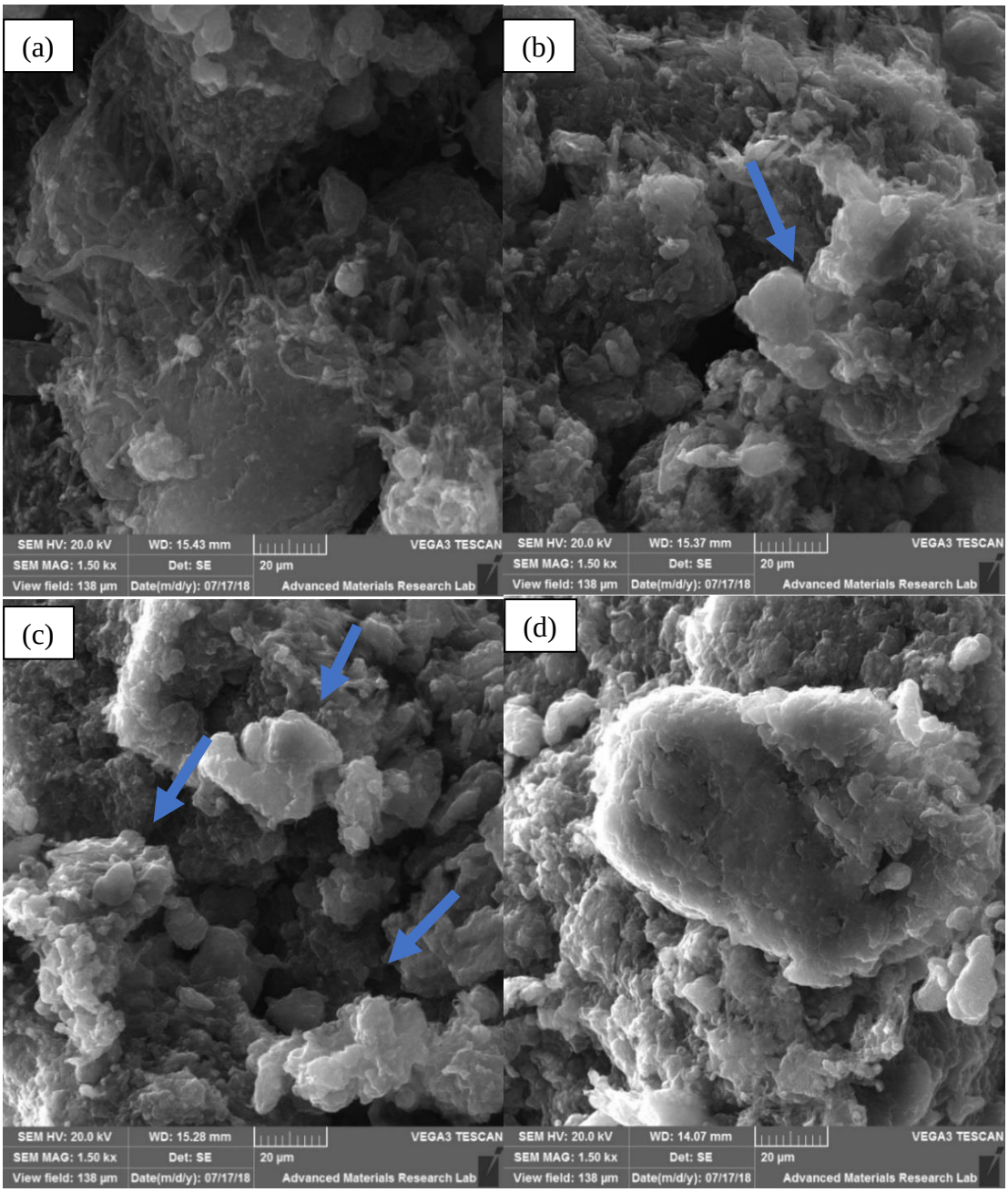

Figure 4.3: SEM result images (a) raw MWCNTs, (b) MWCNTs-CTAB, (c) MWCNTs-CTAB after adsorption of Cr(VI), (d) MWCNTs-CTAB-Cr(VI) after regeneration using KCl at 25 ^{o}C

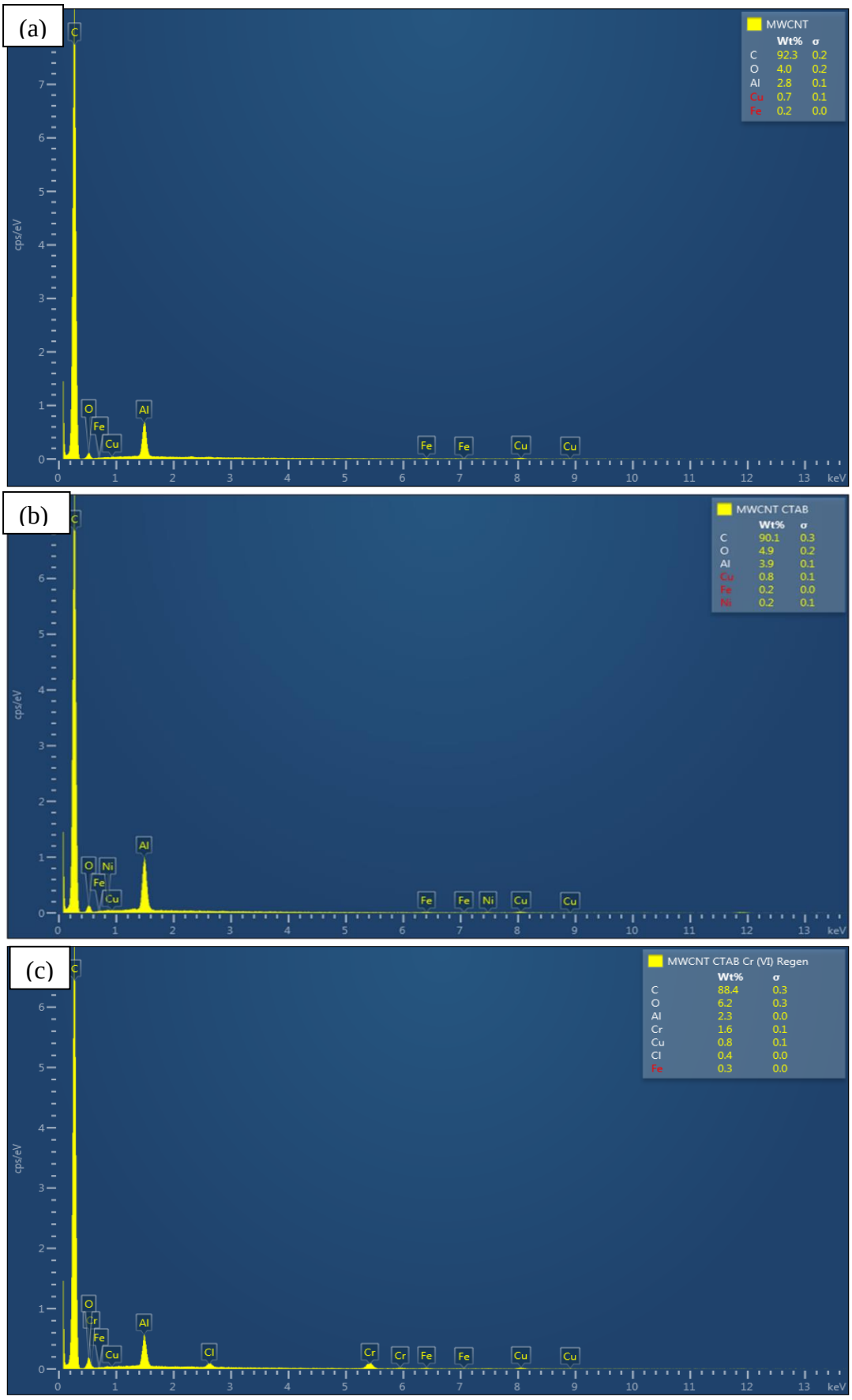

Figure 4.4: EDS analysis of (a) raw MWCNTs, (b) MWCNTs-CTAB, (c) MWCNTs-CTAB after adsorption of Cr(VI)

4.3. Adsorption Parameters Optimization

4.3.1. Effect of adsorbents dosage. The study of adsorbent dosage is one of the most important factors to study during adsorption for it directly affect the number of sites available for adsorption. The effect of dosage on the removal efficiency of MWCNTs-CTAB is shown in Figure 4.5. The study was performed at pH 2 of a 10 mL of 100 ppm Cr(VI) solution. The dosage of MWCNTs-CTAB was varied from 0.01 g to 0.08 g. The samples were kept in a temperature-controlled shaker for a contact time of 120 min, a temperature of 25 ^{o}C and shaking speed of 150 rpm. The removal efficiency was noticed to be increase when the dosage increased which is due to the increase in the adsorption sites available for adsorption. It is also noted that beyond adsorbent dosage of 0.05 g the removal becomes almost constant at a value of 98 ± 1%. Therefore, the optimum dosage for the adsorption study was selected to be 0.05 g**.**

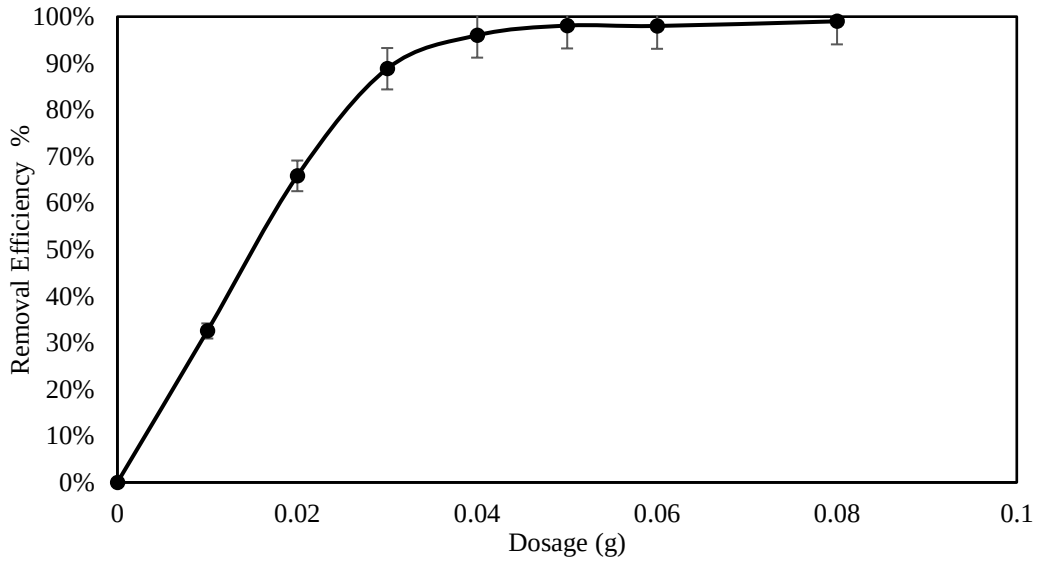

Figure 4.5: Effect of adsorbent dosage on the removal of Cr(VI) from aqueous solution for MWCNTs-CTAB at contact time = 120 min, pH = 2 ± 0.05, temperature = 25 ± 2 ^{o}C, initial concentration = 100 ppm and shaking rate = 150 rpm.

4.3.2. Effect of pH. The pH of the solution can affect the adsorbent surface charge, speciation of Cr(VI) and concentration of hydrogen and hydroxyl ions; which can act as a competing ion during adsorption [84]. In aqueous mediums, Cr(VI) is not always a simple monovalent anion but rather a series of chromate anions depending upon the pH and concentration of the solution as explained in subsection 2.5 [85]. In acid solutions, Cr(VI) mainly exists as hydrogen chromate, $HCrO_4^-$, which is expected to bind more easily at the positively charged surface of modified MWCNTs-CTAB [84,

86]. However, as pH increases $HCrO_4^-$ constantly converts to CrO_4^{2-} and $Cr_2O_7^{2-}$ which would weaken the ability of Cr(VI) to bind to the adsorbent surface [85]. For adsorption purposes, acidic pH is favored; therefore, the effect of pH was studied in the range of 1 – 6 and the removal efficiency was obtained accordingly. 100 ppm of Cr(VI) solution was prepared and placed in 10 mL solution containing 0.05 g MWCNTs-CTAB. The samples were shaken in a temperature-controlled shaker for 120 min at a temperature of 25 ^oC and speed rate of 150 rpm. Figure 4.6 shows the results obtained. Results revealed that as the pH increased above 5, the removal efficiency decreased. A constant high removal efficiency of 97 - 99% was obtained at a pH of 1 to 5 and a relatively low removal of 89% was obtained at pH of 6. The lower efficiency obtained at pH 6 can be due to the competing hydroxyl ion that exists at higher pH values and the ability of Cr(VI) to speciation into stable ions. From the obtained findings, a pH of 4.5 was selected as an optimum pH for adsorption study, due to high removal efficiency achieved and less chemical reagent dependency for pH adjustments.

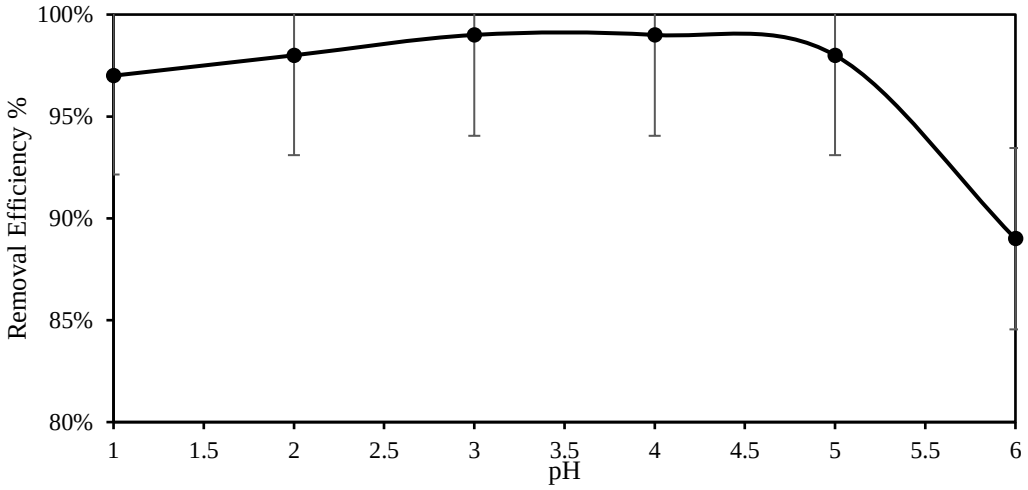

Figure 4.6: Effect of pH on the removal of Cr(VI) from aqueous solution for MWCNTs-CTAB at contact time = 120 min, initial concentration = 100 ppm, temperature = 25 ± 2 ^oC, adsorbent dosage = 0.05 g, and shaking rate = 150 rpm.

4.3.3. Effect of contact time. The study of the effect of contact time during adsorption is another important parameter to study in order to ensure sufficient time for adsorption equilibrium to be achieved. Effect of contact time on the removal efficiency was studied by changing the contact time from 7 min to 120 min while keeping pH, temperature, initial concentration and shaking rate constant. Results of the effect of contact time on the removal efficiency of Cr(VI) is presented in Figure 4.7. The figure shows that Cr(VI) was adsorbed during the first 7 min this is due to the empty

adsorption sites available. As the contact time increased the available adsorption sites got occupied by Cr(VI) and caused the removal efficiency rate to be lowered. Equilibrium was reached after 30 min where a constant removal efficiency of 98% was achieved and therefore, was selected as optimum contact time for adsorption. Similar results were reported also in other studies, where adsorption on MWCNTs was fast and equilibrium was achieved in the first 30 min [74, 87]. Thus, it can be concluded that results obtained from this study are in accordance with previous reported studies.

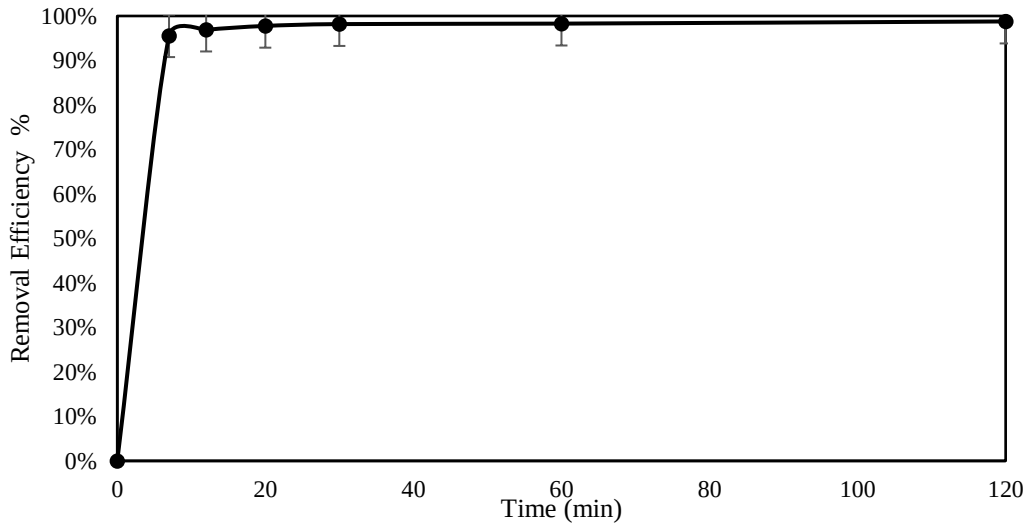

Figure 4.7: Effect of contact time on the removal of Cr(VI) from aqueous solution for MWCNTs-CTAB at pH = 4.5, initial concentration = 100 ppm, temperature = 25 ^{o}C, adsorbent dosage = 0.05 g, and shaking rate = 150 rpm.

4.3.4. Effect of temperature. In order to study the effect of temperature on Cr(VI) adsorption, experimental studies at temperatures of 25 ^{o}C, 30 ^{o}C and 35 ^{o}C were conducted at the optimum conditions of a dosage of 0.05 g, pH of 4.5 and contact time of 30 min. Figure 4.8 shows the effect of temperature on the removal efficiency of Cr(VI) using MWCNTs-CTAB. The removal efficiencies obtained as a result of effect of temperature show no significant increase in removal, 0.56% greater than the removal obtained at 25 ^{o}C. Thus, 25 ^{o}C was chosen to be the optimum temperature and was used in further studies.

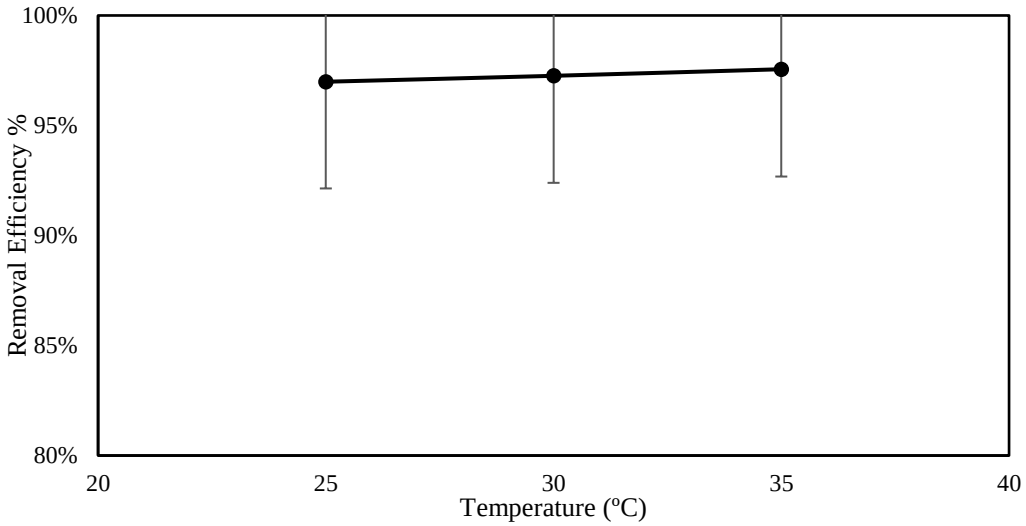

Figure 4.8: Effect of temperature on the removal of Cr(VI) from aqueous solution for MWCNTs-CTAB at pH = 4.5 ± 0.05, initial concentration= 100 ppm, contact time = 30 min, adsorbent dosage = 0.05 g, and shaking rate = 150 rpm.

4.4. Adsorption Equilibrium Isotherms

The study of initial concentration of Cr(VI) at selected optimum equilibrium conditions is essential to study effectiveness of the proposed adsorption process. Cr(VI) solutions with different initial metal concentration, fixed pH, contact time, temperature, and adsorption dosage were used to study the adsorption equilibrium. Adsorption capacity was calculated using Equation (26):

$$q_e = \frac{C_o - C_e}{m} * V \tag{26}$$

where q_e is the equilibrium adsorption capacity (mg/g), C_o and C_e are the initial and equilibrium concentrations in (ppm), respectively. V is the volume of solution (mL) and m is the mass of adsorbent (g). The removal percent efficiency versus initial concentration is plotted in Figure 4.9 which shows that the removal efficiency decreased as the initial concentration increased. This phenomenon is due to the limited number of adsorption sites available for adsorption, since the quantity of adsorbent was fixed at 0.05 g, the number of active adsorption sites remained constant. These sites eventually become saturated and are unable to accommodate any more ions at higher concentrations. The lowest efficiency achieved from this study is at initial concentration of 500 ppm with 28% removal of Cr(VI). The adsorption capacity versus initial concentration is given in Figure 4.10. The adsorption capacity for MWCNTs-CTAB was seen to reach maximum at around 30 mg/g at approximately 400 ppm initial concentration and then decrease exponentially to a value of 27.3 mg/g at 500 ppm. The

equilibrium data of MWCNTs-CTAB were fitted to different isotherms models which include Langmuir, Freundlich, Temkin, D-R and Sips. Equations of these models are presented in subsection 0. The isotherm model which best describe this study was determined. The best fit for the two parameters isotherm will be selected based on the highest coefficient of determination (R^2) value. The best fit for three parameters model, Sips, is obtained using an error function assessment. Sum of Square Errors (SSE) was used as the error function and was minimized using Microsoft's add-in, "solver" to find the best theoretical adsorption capacity values for this adsorption study, SSE equation is given in Equation (27). Results of data fitting on Langmuir, Freundlich, Temkin, D-R and Sips are shown in Figure 4.11 to Figure 4.15. R^2 and SSE values along with the respective model's key parameters are summarized in Table 4.3.

$$SSE = \sum\left(Q_{exp} - Q_{theo}\right)^2 \quad (27)$$

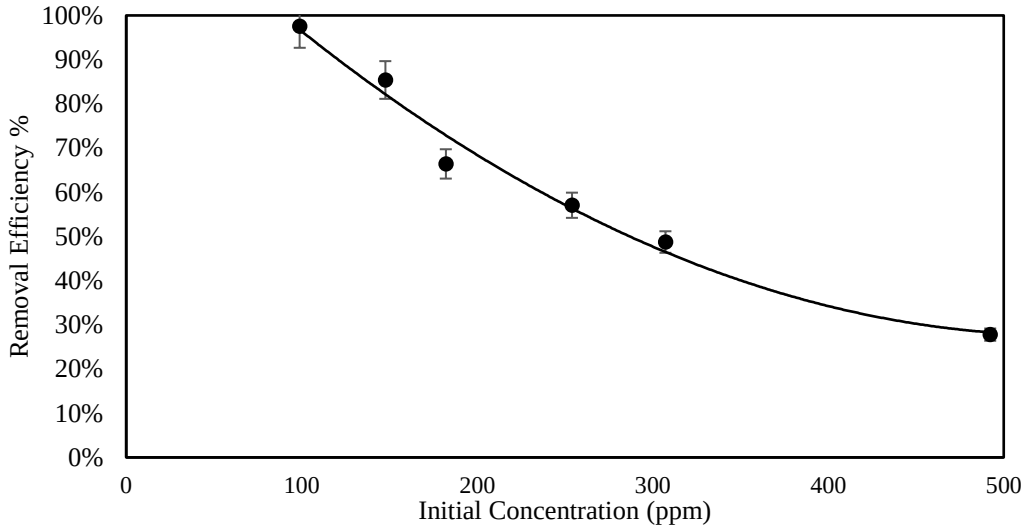

Figure 4.9: Change in removal efficiency with initial concentration using MWCNTs-CTAB, at adsorbent dosage = 0.05 g, contact time = 30 min, pH = 4.5 ± 0.05, temperature = 25 ± 2 ^oC and shaking time = 150 rpm

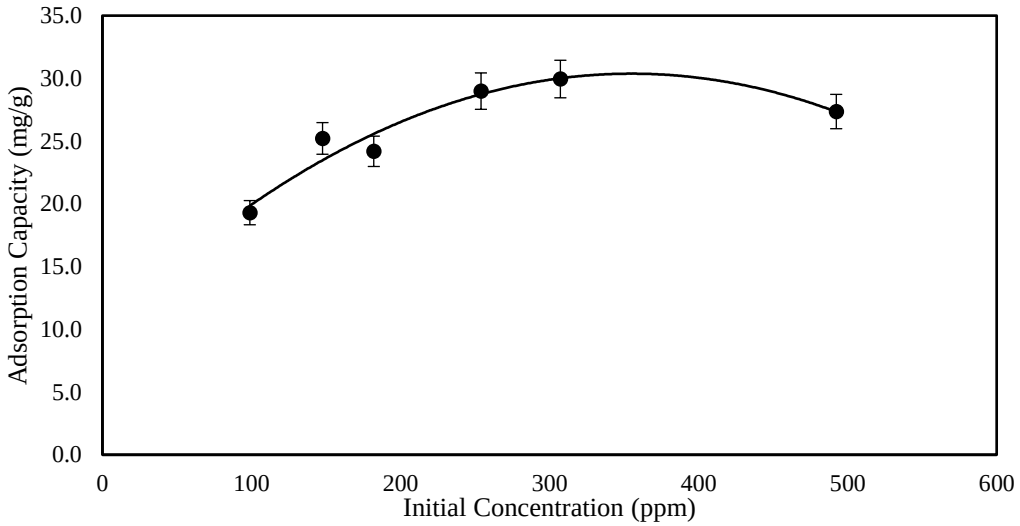

Figure 4.10: Change in adsorption capacity with initial concentration using MWCNTs-CTAB at adsorbent dosage = 0.05 g, contact time = 30 min, pH = 4.5 ± 0.04, temperature= 25 ± 2 ^{o}C and shaking time = 150 rpm

4.4.1. Langmuir isotherm model. Langmuir isotherm generally describes the formation of adsorbent on the outer surface of the adsorbent with no further adsorption. It is valid only for monolayer adsorption on a finite number of sites. R^2 obtained for this isotherm for Cr(VI) adsorption on MWCNTs-CTAB, shown in Figure 4.11, is 0.9968 which is the highest compared to the other models. This suggests that Langmuir model is the best model for describing adsorption of Cr(VI) on MWCNTs-CTAB. The maximum adsorption capacity of MWCNTs-CTAB calculated from this model is 27.78 mg/g. Since Langmuir model is the best fit for adsorption of Cr(VI) on MWCNTs-CTAB; it can be concluded that the adsorption is monolayer and reversible [36]. R_L value of 0.0025 was obtained for this study; as explained in subsection 0 where values < 0 mean that adsorption is favorable.

4.4.2. Freundlich isotherm model. The obtained R^2 for the adsorption of Cr(VI) on MWCNTs-CTAB using Freundlich isotherm, shown in Figure 4.12, is a 0.7983 which indicates that this model does not represent the proposed adsorption process.

4.4.3. Temkin isotherm model. The obtained R^2 for the adsorption of Cr(VI) on MWCNTs-CTAB using Temkin isotherm model, shown in Figure 4.13, is 0.7731 which is the second lowest listed after Freundlich isotherm and before D-R. The

low R^2 indicates that this model is not representative of the adsorption of Cr(VI) on MWCNTs-CTAB [36, 37].

4.4.4. Dubinin–Radushkevich (D-R) isotherm model. The obtained R^2 for the adsorption of Cr(VI) on MWCNTs-CTAB using D-R model is the lowest in comparison to Temkin, Freundlich and Langmuir models with a value of 0.7512, results shown in Figure 4.14. D-R model is generally used to describe adsorption of subcritical vapors onto micropore solids which does not represent the adsorption of Cr(VI) on MWCNTs-CTAB [36, 42]. Comparing the obtained R^2 values of all the fitted two parameters isotherm models, it indicates that Langmuir isotherm model best describes this adsorption study of Cr(VI) removal using surface modified MWCNTs-CTAB.

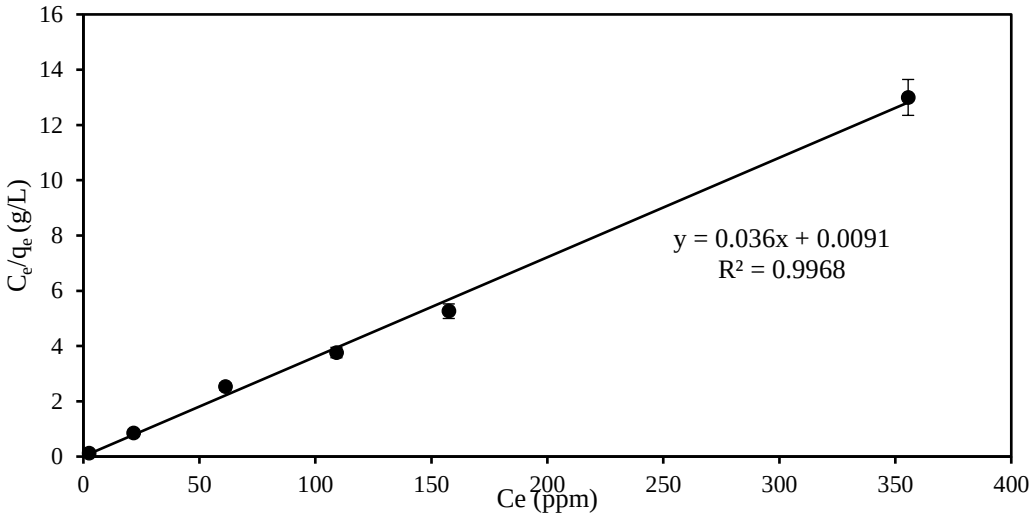

Figure 4.11: Langmuir isotherm model for adsorption of Cr(VI) on MWCNTs-CTAB

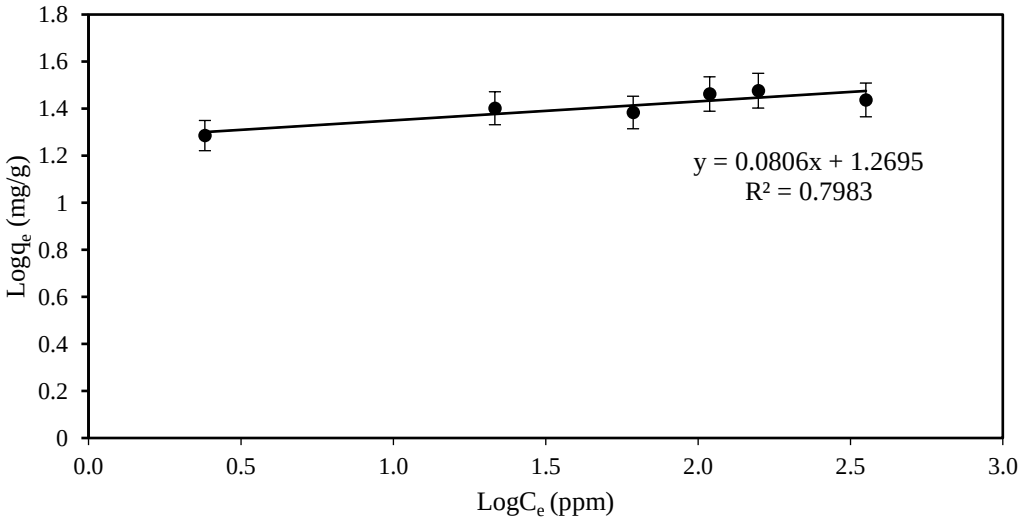

Figure 4.12: Freundlich isotherm model for adsorption of Cr(VI) using MWCNTs-CTAB

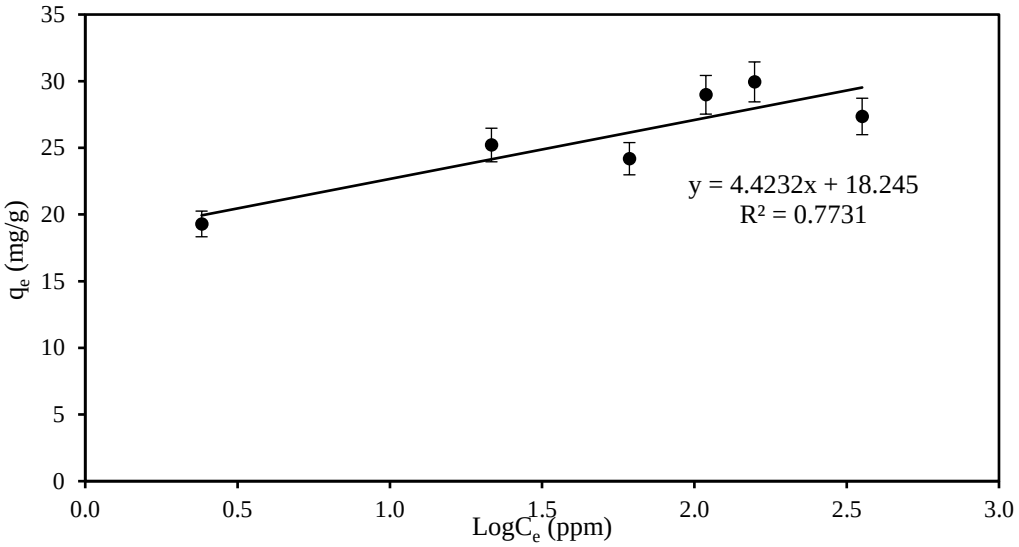

Figure 4.13: Temkin isotherm model for adsorption of Cr(VI) using MWCNTs-CTAB

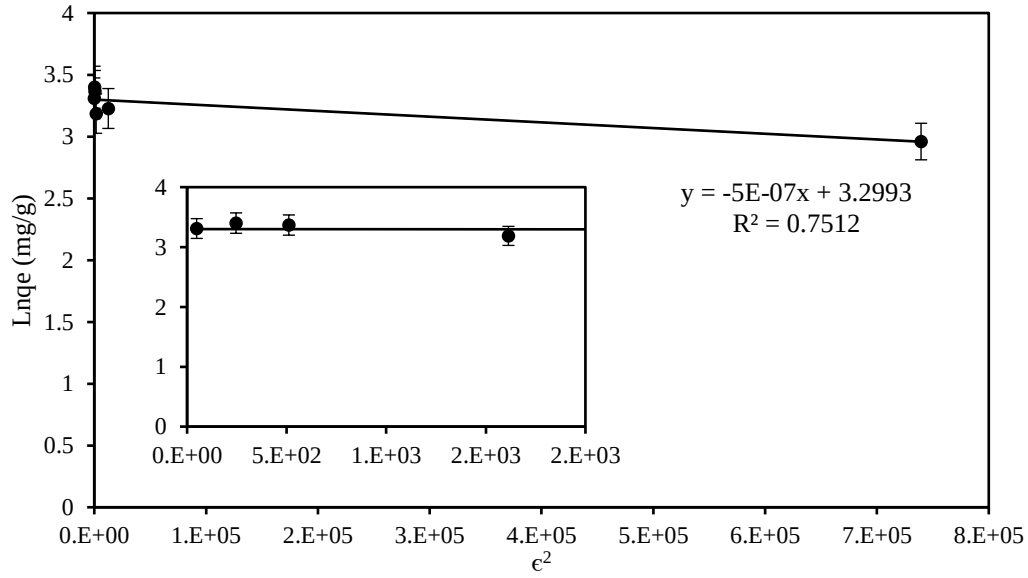

Figure 4.14: D-R isotherm model for adsorption of Cr(VI) using MWCNTs-CTAB

4.4.5. Sips isotherm model. Sips isotherm model, an empirical three parameters isotherm model, was plotted as equilibrium concentration versus theoretical adsorption capacity. For the case where $K_e C_e$ is much less than 1, Sips equation is reduced to Equation (28) which was used to calculate Sips parameters n_s, K_e and $q^e_{th,m}$. The derived used equation is called Freundlich-type sips isotherm. The SSE obtained value was 18.71 for 6 experimental parameters. The linear fit of the theoretical values provided an $R^2 = 1$. The theoretical adsorption capacity obtained from Sips isotherm

model is 25.688 mg/g which is very close to the value obtained using Langmuir isotherm model.

$$q_e = q_{th,m}^{e} K_e C_e^{n_s} \tag{28}$$

The adsorption capacity of MWCNTs-CTAB which is used for this study was best represented using Langmuir isotherm model. Parameters and results of all the isotherm models obtained and fitted are summarized in Table 4.3. The value of adsorption capacity was found to be 27.78 mg/g highest in comparison to other fitted isotherm models in this study. Generally, different modification techniques and modification complexity will allow for different functional groups to be attached on the surface of MWCNTs which can directly affect their adsorption capacity. Adsorption capacities of differently modified MWCNTs for the removal of Cr(VI) from aqueous solution are shown in Table 4.4.

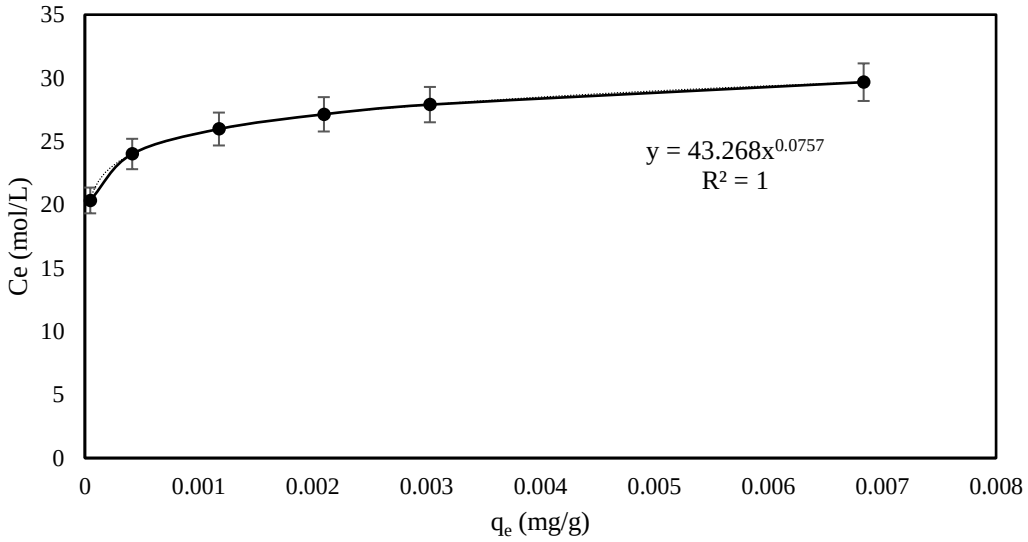

Figure 4.15: Sips isotherm model for adsorption of Cr(VI) using MWCNTs-CTAB

4.5. Adsorption Kinetics

Adsorption kinetics is an essential study in adsorption process. This study can determine the rate of the proposed adsorption process. Adsorption kinetics information are used to determine adsorption residence time and adsorption design characteristics. In this study, adsorption of Cr(VI) on MWCNTs-CTAB is fitted to pseudo- first order model, pseudo- second order model and Elovich model and the obtained results are shown in Figure 4.16 to Figure 4.18.

Table 4.3: Adsorption isotherm parameters for the five models for Cr(VI) removal using MWCNTs-CTAB

Adsorption Isotherm	Parameters	R^2
Langmuir	Q_m = 27.7 mg/g K_L = 3.956 L/mg	0.9968
Freundlich	n = 12.4 K_f = 18.6 ($mg^{1-1/n}.L^{1/n}$)/g	0.7983
Temkin	A_T = 13330.36 L/g B = 4.4232 J/mol B = 560.131	0.7731
D-R	q_s = 27.5 mg/g K_{ad} = $5*10^{-7}$ mol^2/kJ^2	0.7512
Sips	K_e= 1.695 n = 0.0757 $q^e_{th,m}$= 25.688 mg/g	SSE = 18.7 R^2 = 1

Table 4.4: Various functional groups MWCNTs adsorption capacities

Functional Group	Adsorbate	Adsorption Capacity (mg/g)	Reference
Magnetic MWCNTs	Cr(VI)	12.53 mg/g	[76]
MWCNTs–Iminodiaceticacid	V(V),Cr(VI), Pb(II),Cd(II), Co(II), Cu(II) and As (III).	8.96 mg/g	[73]
Unmodified MWCNTs	Cr(VI)	1.26 mg/g	[24]
Unfunctionalized MWCNTs synthesized using CVD	Cr(VI)	60.98 mg/g	[19]
Functionalized MWCNT with hydroxyl and carboxyl	Cr(VI)	41.16 mg/g	[19]
Polyethyleneimine-MWCNTs polymeric nanocomposite	Cr(VI)	40.30 mg/g	[88]
Chitosan/MWCNTs/Fe_3O_4 nanofibrous	Cr(VI)	335.60 mg/g	[87]
Nitric acid oxidized MWCNTs	Cr(VI)	4.26 mg/g	[89]

Table 4.5: Adsorption Kinetics Model Parameters

Adsorption kinetics model	Parameters	R^2
Pseudo- first order	k_1 = 0.147 min^{-1}	0.533
Pseudo- second order	k_2 = $9.85*10^{-4}$ g/mg.min	0.999
Elovich	α = $3.45*10^{-8}$ mg/g.min β = 0.57 g/mg	0.823

Pseudo first- order equation assumes a linear driving force of a nonreversible adsorption process [90, 91]. Pseudo- first order has five assumption which are the following:

1) Adsorption only occurs on localized sites and involves no interaction between the adsorbed ions.
2) The energy of adsorption is not dependent on surface coverage.
3) Maximum adsorption corresponds to a saturated monolayer of adsorbates on the adsorbent surface.
4) The concentration of adsorbate is considered to be constant.
5) The metal ion uptake on the activated carbons is governed by a first order rate equation.

Pseudo- second order is similar to pseudo- first order however, it assumes the adsorption is not linear but to the power of two.

Lastly, Elovich model is similar to pseudo- first order but has few alterations which are:

1) Adsorption only occurs on localized sites and there is interaction between the adsorbed ions.
2) The energy of adsorption increases linearly with the surface coverage
3) The metal ion uptake on the activated carbons is negligible before the exponential

Equations for the three kinetic models explained are given in subsection 2.7.2. Table 4.5 provides the values of the calculated R^2 and the obtained rate parameters for three studied kinetic models. From the R^2 values, it can be concluded that adsorption of Cr(VI) on MWCNTs-CTAB is best fitted to pseudo- second order model. R^2 values were found to be equal to approximately 1. Thus, it can be concluded the adsorption of Cr(VI) ions on the surface of MWCNTs-CTAB is governed by pseudo- second order rate equation. Similar findings were reported in previous experimental studies [71, 72, 73, 37, 24] in which MWCNTs was used with different functional group.

4.6. Adsorption Mechanism

Adsorption mechanism models are generally used to determine the rate controlling step in a proposed adsorption process. Intraparticle and film diffusion models are used to study adsorption mechanism. The best fit model is selected by obtaining and comparing R^2 values. The obtained fit for intraparticle and film diffusion

models is shown in Figure 4.19 and Figure 4.20, respectively. Figure 4.19 shows intraparticle diffusion model where the plot has a linear line, but the line does not pass through the origin which means there are other mechanisms contributing in the limiting step other than the intraparticle diffusion [92]. Film diffusion model, shown in Figure 4.20, also does not pass through the origin which means that film diffusion is not the limiting step in the adsorption process. The R^2 value for intraparticle diffusion is higher than film diffusion model but is not the rate limiting step in the proposed adsorption study.

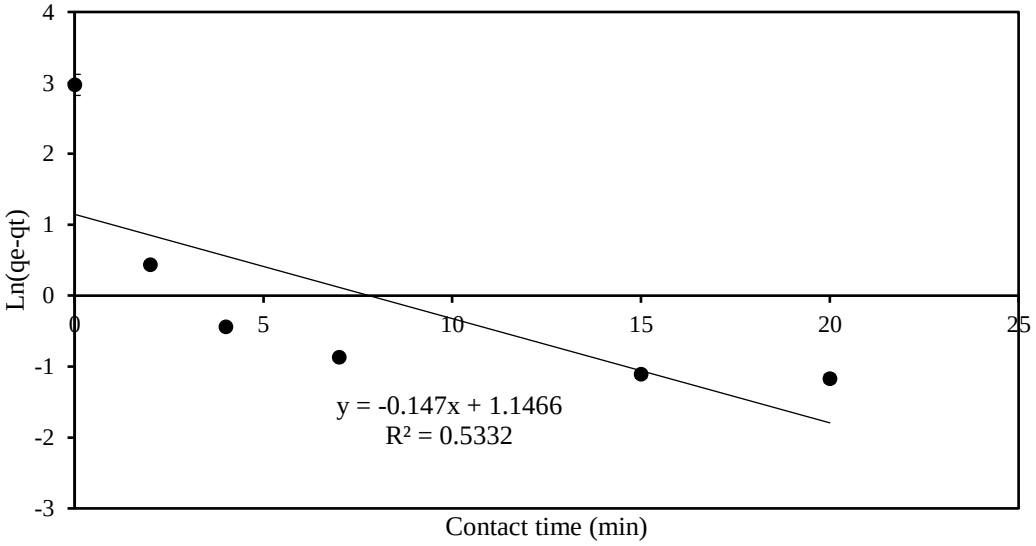

Figure 4.16: Pseudo- first order model for adsorption of Cr(VI) using MWCNTs-CTAB

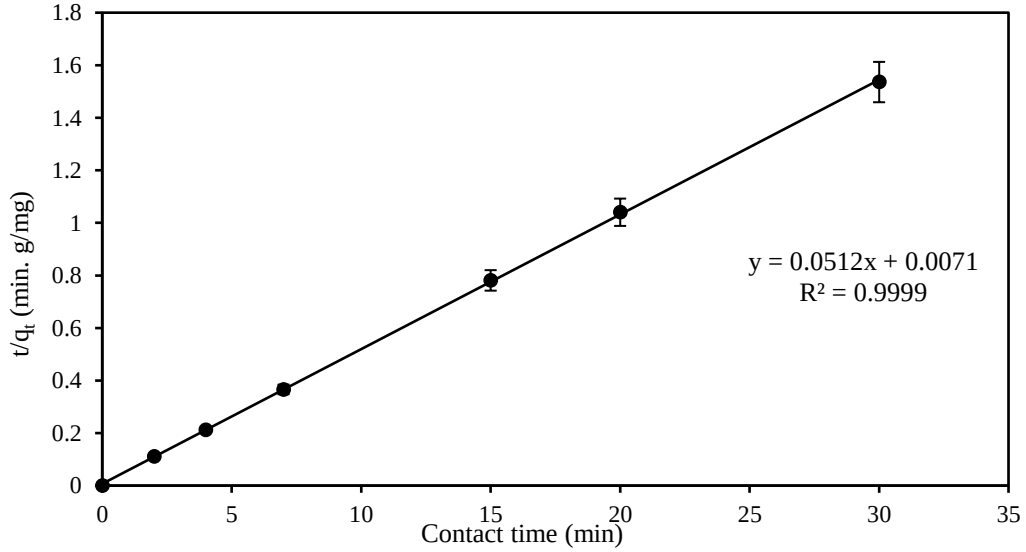

Figure 4.17: Pseudo- second order model for adsorption of Cr(VI) using MWCNTs-CTAB

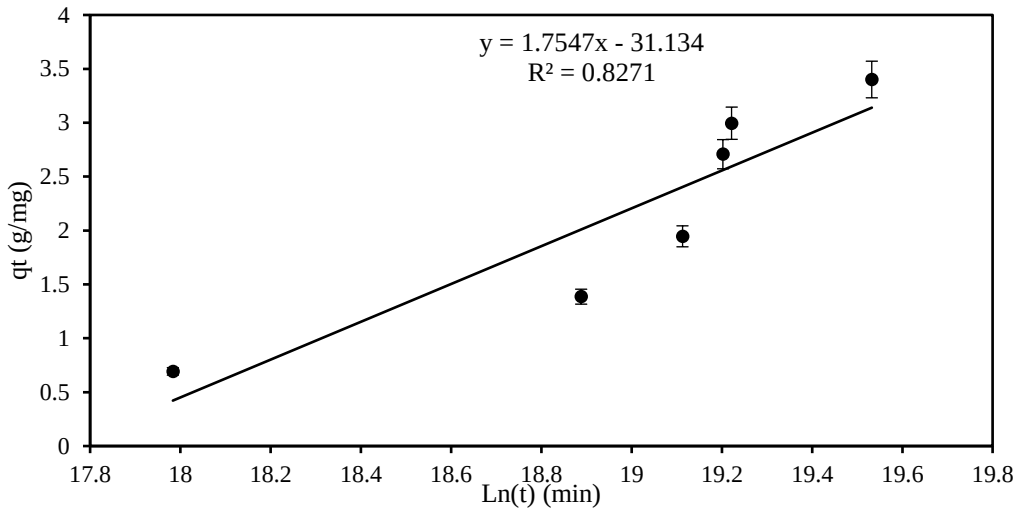

Figure 4.18: Elovich model for adsorption of Cr(VI) using MWCNTs-CTAB

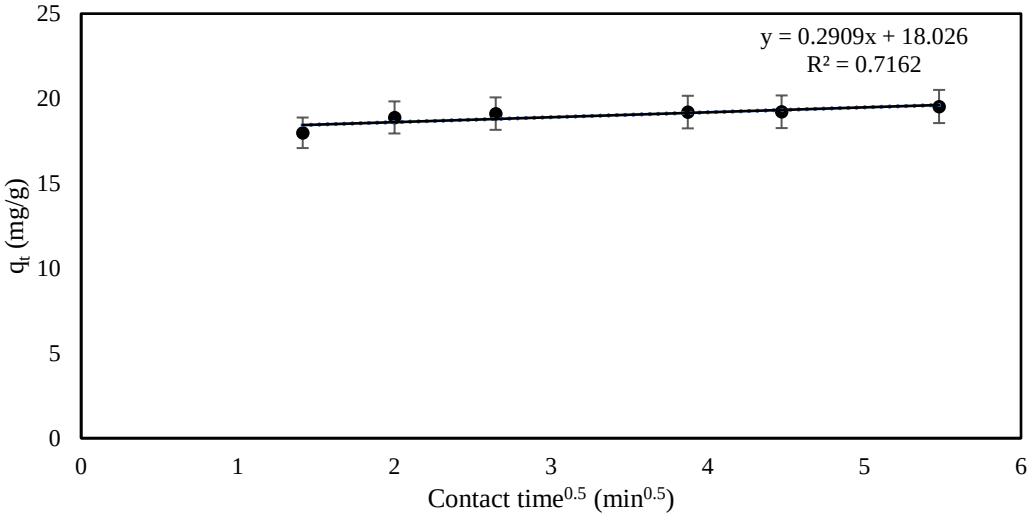

Figure 4.19: Intraparticle diffusion model for Cr(VI) adsorption using MWCNTs-CTAB

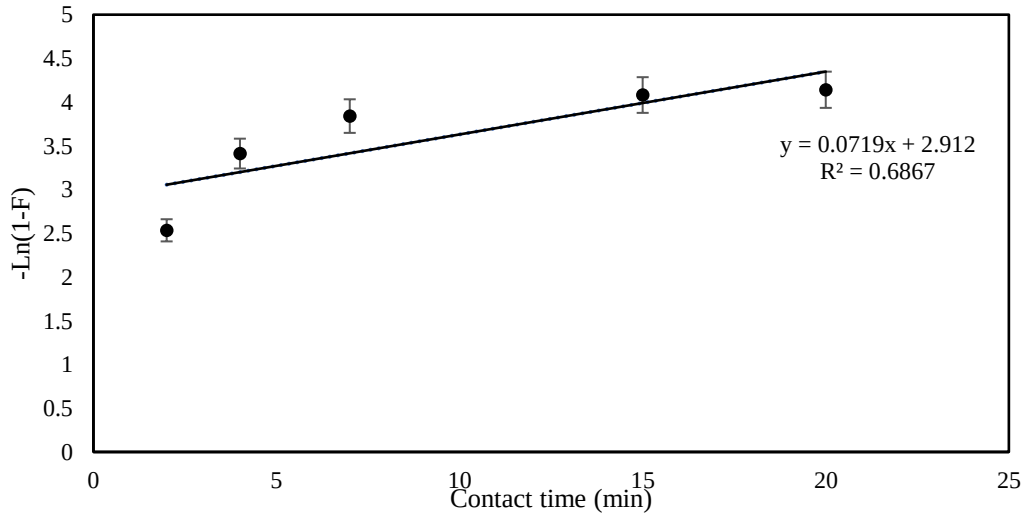

Figure 4.20: Film diffusion model for Cr(VI) adsorption using MWCNTs-CTAB

4.7. Adsorption Thermodynamics

Various thermodynamic parameters are obtained to fully understand any adsorption process. Parameters such as Gibbs free energy change (ΔG), enthalpy change (ΔH) and entropy change (ΔS) are calculated for the adsorption of Cr(VI) on MWCNTs-CTAB. The values of K_e were obtained using derived Sip's equation for four temperatures 25 °C, 30 °C, 35 °C, 45 °C and the values of n_s, K_e, $q^e_{th,m}$ and ΔG were calculated and are presented in Table 4.6. ΔH and ΔS values are obtained from Van't Hoff plot of $ln\, K_e$ versus T^{-1} and is shown in Figure 4.21. ΔG values between −20.0 kJ/mol and 0 kJ/mol indicate physisorption processes; whereas, for chemisorption processes, the range of ΔG is between −400 kJ/mol and −80.0 kJ/mol [35]. The calculated values of ΔG for this study were within −20 to 0 kJ/mol (Table 4.6), which means the process is physical for all temperatures. In addition, the negative sign of the calculated ΔG indicate a spontaneous nature of the process. The calculated ΔH value for this study is 14.06 kJ/mol, in which the positive sign indicates an endothermic behavior of the adsorption process. Lastly, ΔS was calculated to be 0.0516 kJ/mol.K and the positive sign indicates the degree of randomness of Cr(VI) and MWCNTs-CTAB boundary during adsorption.

Table 4.6: Thermodynamic parameters fitted to Sips Equation

Temperature	K_e	$q^e_{th,m}$ (mg/g)	n_s	$K_f = Q^e_{th,m}K_e$	ΔG(kJ/mol)
25 °C	1.684	25.688	0.076	43.268	-1.30
30 °C	1.897	24.773	0.087	47.000	-1.60
35 °C	2.035	21.536	0.077	43.823	-1.76
45 °C	2.463	17.675	0.081	43.533	-2.23

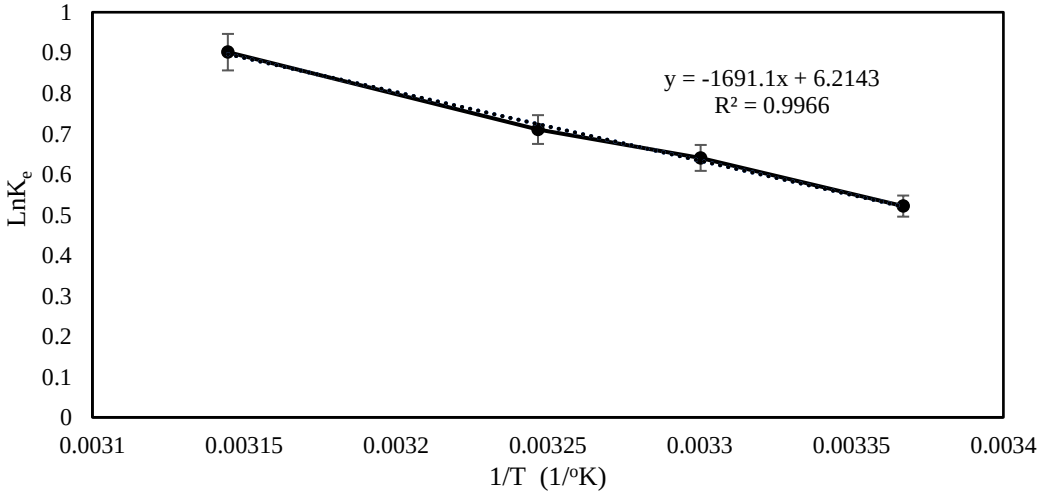

Figure 4.21: Van't Hoff plot of LnK_e versus 1/T for the adsorption of Cr(VI) using MWCNTs-CTAB

4.8. Regeneration

Regeneration was completed on Cr(VI) saturated MWCNTs-CTAB using the procedure described in subsection 3.3.4. The results of two regeneration-adsorption cycles are shown in Figure 4.22 and Figure 4.23 for a regeneration temperatures of 25 ^{o}C and 35 ^{o}C, respectively. The adsorption efficiency dropped from 98% to 73% and from 73% to 60% for samples regenerated at a temperature of 25 ^{o}C. The adsorption efficiency dropped from 98% to 75% and from 75% to 61% for samples regenerated at a temperature of 35 ^{o}C. From this study, it can be concluded that the regeneration temperature did not heavily alter the adsorption efficiency of the regenerated samples however, samples regenerated at 35 ^{o}C were slightly more effective. The regeneration study indicated that the regeneration reagent or regeneration method needs to be studied more thoroughly to allow the adsorption efficiency of MWCNTs-CTAB to remain high with tolerable losses.

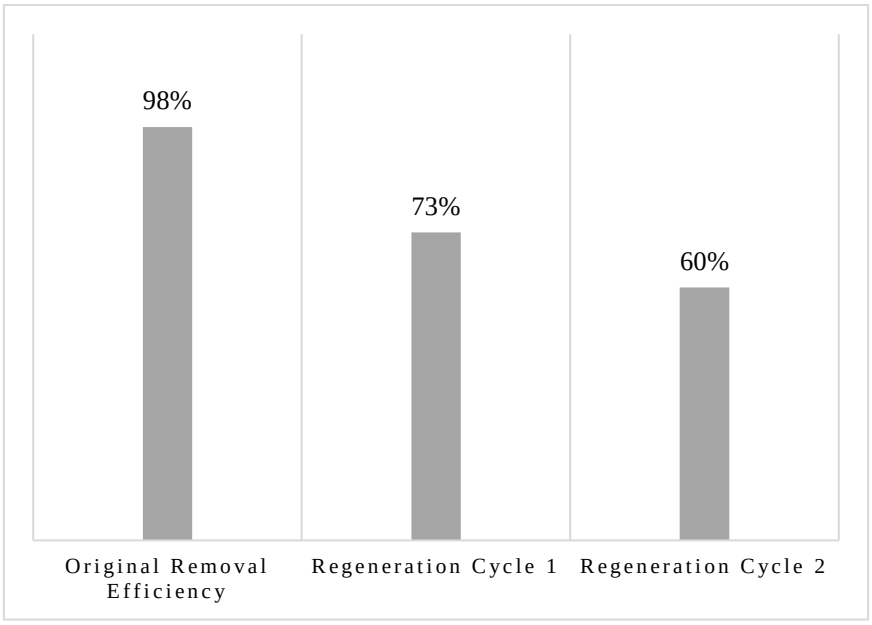

Figure 4.22: Removal efficiencies of Cr(VI) using regenerated MWCNTs-CTAB at regeneration temperature = 25 ± 2 ^{o}C and regeneration solution = 0.1 M KCl. Adsorption cycle 1 & 2 were at pH = 4.5 ± 0.05, initial concentration = 100ppm, contact time = 30 min, adsorbent dosage = 0.5 g, and shaking rate = 150 rpm

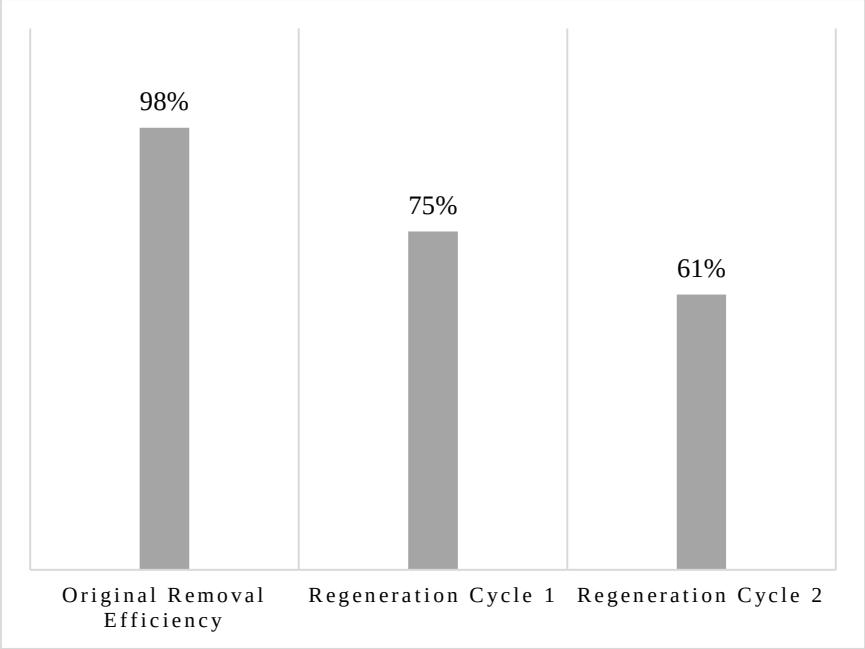

Figure 4.23: Removal efficiencies of Cr(VI) using regenerated MWCNTs-CTAB at regeneration temperature = 35 ± 2 ºC and regeneration solution = 0.1 M KCl. Adsorption cycle 1 & 2 were at pH = 4.5 ± 0.05, initial concentration = 100 ppm, contact time = 30 min, adsorbent dosage = 0.5 g, and shaking rate = 150 rpm

Chapter 5. Conclusions and Recommendations

In this study, various heavy metals along with their sources, adverse effects, laws and regulations were discussed. Hexavalent chromium [Cr(VI)] was selected as the studied heavy metal in this thesis. Several techniques used for the removal of heavy metals from wastewater were discussed. Adsorption process was thoroughly reviewed through a comprehensive study of adsorption isotherms, adsorption kinetics, adsorption mechanisms and adsorption thermodynamics. Adsorption was selected as an optimum treatment technique for the removal of Cr(VI) from wastewater due to its simplicity, relatively low capital cost, low operational cost and reusability. Adsorbents commonly used in wastewater adsorption processes were reviewed. Carbon nanotubes (CNTs) were selected as an ideal adsorbent for this study. Benefits and drawbacks of using CNTs were discussed along with their well-explored synthesis methods, properties, applications and functionalization techniques.

This thesis examined a surface modified multiwall carbon nanotubes (MWCNTs) for removal of Cr(VI) from wastewater. The surface of MWCNTs was physically modified with a cationic surfactant which is cetyl trimethylammonium bromide (CTAB) to form MWCNTs-CTAB complex. MWCNTs-CTAB were characterized using TGA, FTIR, SEM and EDS. Results show that the surface of MWCNTs was successfully modified with the selected surfactant, CTAB. Adsorption study using MWCNTs-CTAB was performed to obtain the adsorption capacity and efficiency. Optimum values in terms of adsorbent dosage, contact time, pH and temperature using MWCNTs-CTAB were found to be 0.05 g, 30 min, 4.5, and 25 ^{o}C, respectively. Langmuir isotherm was found to be the best fit isotherm model, where it provided a maximum adsorption capacity of 27.78 mg/g. Furthermore, kinetic study revealed that MWCNTs-CTAB followed pseudo- second order kinetic model with a rate constant of $9.85*10^{-4}$ g/mg.min. In addition, the thermodynamic study indicated that the adsorption of Cr(VI) is an endothermic process. The regeneration study on saturated MWCNTs-CTAB was performed at two regeneration temperatures, 25 ^{o}C and 35 ^{o}C, in two cycles of desorption-adsorption. The regeneration solution used was 0.1 M potassium chloride (KCl). Results for the samples regenerated at 25 ^{o}C revealed that the removal efficiency dropped from 98% to 73% to 60%. Similarly, samples regenerated at 35 ^{o}C the removal efficiency dropped from 98% to 75% to 61%.

From this batch experimental study, it can be concluded that the removal of Cr(VI) from wastewater using MWCNTs-CTAB was successful in which a removal

efficiency of 98% was achieved at the selected optimum conditions. However, the adopted regeneration method used during this study is deemed inadequate as the removal efficiencies of the regenerated samples were not as high as the original sample. Therefore, it is recommended to find a more suitable and efficient method for the regeneration of saturated MWCNTs-CTAB samples. Thorough studies of regeneration contact time, regeneration reagent and regeneration concentration are recommended to find the most optimum method to regenerate the obtained samples.

References

[1] L. I. Simeonov, M. V. Kochubovski and B. G. Simeonova, *Environmental Heavy Metals and Mental Disorders*, Springer, 2011.

[2] B. D. and M. Petrovic, "Waste Water Treatment and Reuse in the Mediterranean Region," in *The Handbook of Environmental Chemistry*, Heidelberg, Springer, 2011, pp. 1-28.

[3] M. Pescod, "Wastewater Treatment," in *Wastewater treatment and use in agriculture*, Italy, FAO, 1992.

[4] Y. El Taweel, E. Nassef, I. Elkheriany and D. Sayed, "Removal of Cr(VI) ions from waste water by electrocoagulation using iron electrode," *Egyptian Journal of Petroleum,* vol. 24, no. 2, pp. 183-192, 2015.

[5] A. S. Kalamdhad and J. Singh, "Effects of Heavy Metals on Soil, Plants, Human Health and Aquatic Life," *International Journal of Research in Chemistry and Environment,* vol. 1, no. 2, pp. 15-21, 2011.

[6] I. A. Ajayi and R. A. Oderinde1, "Evaluation of Selected Heavy Metals and Macronutrients Status," *Journal of Pharmacy and Biological Sciences,* vol. 8, no. 2, pp. 12-17, 2013.

[7] B. Vigon, R. Craig and N. Frazier, "The sources and behavior of Heavy Metals in Wastewater and Sludges," U.S. Environmental Protection Agency, Washington, D.C., 1977.

[8] D. Song, K. Pan, A. Tariq, A. Azizullah, F. Sun, Z. Li and Q. Xiong, "Adsorptive Removal of Toxic Chromium from Waste-Water using Wheat Straw and Eupatorium adenophorum," *PLoS ONE,* vol. 11, no. 12, pp. e0167037, 2016.

[9] P. B. Tchounwou, C. G. Yedjou, A. K. Patlolla and D. J. Sutton, "Heavy Metals Toxicity and the Environment," *EXS,* vol. 101, pp. 133–164, 2012.

[10] P. Lahot and D. Tiwari, "Removal of heavy metal ions from industrial wastewater-Review," *Journal of Research in Science, Technology, Engineering and Management (JoRSTEM),* vol. 2, no. 1, pp. 407-418, 2016.

[11] China Water Risk Corporation, "China Water Risk," [Online]. Available: http://chinawaterrisk.org/wp-content/uploads/2011/05/Maximum-Allowable-

Discharge-Concentrations-for-Heavy-Metals-in-China.pdf. [Accessed 2018 May 13].

[12] D. Sud, G. Mahajan and M. Kaur, "Agricultural waste material as potential adsorbent for sequestering heavy metal ions from aqueous solutions – A review," *Bioresource Technology,* vol. 99, no. 14, pp. 6017-6027, 2008.

[13] D. A. John Wase, *Biosorbents for Metal Ions*, 1 ed., J. Wase and C. Forster, Eds., CRC Press, 1997.

[14] United States Environmental Protection Agency, "EPA," [Online]. Available: https://www.epa.gov/ground-water-and-drinking-water/national-primary-drinking-water-regulations#Inorganic. [Accessed 09 September 2018].

[15] Lenntech, "WHO's drinking water standards," [Online]. Available: https://www.lenntech.nl/toepassingen/drinkwater/normen/who-s-drinking-water-standards.htm. [Accessed 2018 September 09].

[16] A. Eatemadi, H. Daraee, H. Karimkhanloo, M. Kouhi, N. Zarghami, A. Akbarzadeh, M. Abasi, Y. Hanifehpour and S. W. Joo, "Discovery, properties and applications of chromium and its compounds," *ChemTexts,* vol. 6, no. 1, 2015.

[17] "Determination of Cr(VI) in Water, Wastewater and Solid Waste Extract," Thermo Fisher Scientific, 2012. [Online]. Available: http://www.dionex-france.com/library/literature/technical_notes/TN26_LPN034398-02.pdf. [Accessed 15 10 2018].

[18] S. Imanaka and H. Hayashi, "Behavior of hexavalent chromium in the water supply system by IC-ICP-MS method," *Water Science & Technology: Water Supply,* vol. 13, no. 1, pp. 96, 2012.

[19] K. Pillay, E. M. Cukrowska and N. J. Coville, "Multi-walled carbon nanotubes as adsorbents for the removal of parts per billion levels of hexavalent chromium from aqueous solution," *Journal of Hazardous Materials,* vol. 166, no. 2–3, pp. 1067-1075, 2009.

[20] "The Trade Effluent Control Regulations 2010," The Regulation and Supervision Bureau for the water, wastewater and electricity sector in the Emirate of Abu Dhabi, Abu Dhabi, 2010.

[21] “Environmental Specifications for Land-Based Liquid Discharges to the Marine Environment,” Abu Dhabi Quality and Conformity Council (QCC), Abu Dhabi, 2017.

[22] F. Fu and Q. Wang, “Removal of heavy metal ions from wastewaters: A review,” *Journal of Environmental Management,* vol. 92, no. 3, pp. 407- 418, 2011.

[23] M. Barakat, “New trends in removing heavy metals from industrial wastewater," Arabian Journal of Chemistry,” *Arabian Journal of Chemistry,* vol. 4, no. 4, pp. 361-377, 2010.

[24] M. Dehghani, M. Taher, A. Bajpai, B. Heibati, I. Tyagi, M. Asif, S. Agarwal and V. Gupta, “Removal of noxious Cr (VI) ions using single-walled carbon nanotubes and multi-walled carbon nanotubes,” *Chemical Engineering Journal,* vol. 279, pp. 344-352, 2015.

[25] T. A. Kurniawan, *Removal of Toxic Cr (VI) from Wastewater*, Nova Science Publishers, 2012.

[26] Minnesota Rural Water Association, “Membrane Filtration,” 2005. [Online]. Available: https://www.mrwa.com/WaterWorksMnl/Chapter%2019%20Membrane%20Filtration.pdf. [Accessed 04 10 2018].

[27] Z. Wang, A. Waag, G. Salamo, N. Kishimoto, S. Bellucci and Y. Park, *Lecture Notes in Nanoscale Science and Technology,* vol. 22, Cham: Springer, 2014.

[28] İ. Duru, D. Ege and A. Kamali, “Graphene oxides for removal of heavy and precious metals from wastewater,” *Journal of Materials Science,* vol. 51, no. 13, pp. 6097-6116, 2016.

[29] I. Enniya, L. Rghioui and A. Jourani, “Adsorption of hexavalent chromium in aqueous solution on activated carbon prepared from apple peels,” *Sustainable Chemistry and Pharmacy,* vol. 7, pp. 9-16, 2018.

[30] M. H. Dehghani, D. Sanaei, I. Ali and A. Bhatnagar, “Removal of chromium (VI) from aqueous solution using treated waste newspaper as a low-cost adsorbent: kinetic modeling and isotherm studies,” *Journal of Molecular Liquids,* vol. 215, pp. 671-679, 2016.

[31] H. N. Bhatti, Q. Zaman, A. Kausar, S. Noreen and M. Iqbal, "Efficient remediation of Zr(IV) using citrus peel waste biomass: Kinetic, equilibrium and thermodynamic studies," *Ecological Engineering,* vol. 95, pp. 216-228, 2016.

[32] V. K. A. S. Gupta and T. A. Saleh, "Synthesis and characterization of alumina-coated carbon nanotubes and their application for lead removal," *Journal of Hazardous Materials,* vol. 185, no. 1, pp. 17-23, 2011.

[33] A. Rashid, H. N. Bhatti, M. Iqbal and S. Noreen, "Fungal biomass composite with bentonite efficiency for nickel and zinc adsorption: A mechanistic study," *Ecological Engineering,* vol. 91, pp. 451-471, 2016.

[34] V. Gupta and A. Nayak, "Cadmium removal and recovery from aqueous solutions by novel adsorbents prepared from orange peel and Fe2O3 nanoparticles," *Chemical Engineering Journal,* vol. 180, pp. 81-90, 2012.

[35] E. Worch, Adsorption Technology in Water Treatment: *Fundamentals, Processes, and Modeling,* Berlin/Boston: De Gruyter, 2017.

[36] A. Dada, A. Olalekan, A. Olatunya and O. Dada, "Langmuir, Freundlich, Temkin and Dubinin–Radushkevich Isotherms Studies of Equilibrium Sorption of Zn2+ Unto Phosphoric Acid Modified Rice Husk," *Journal of Applied Chemistry,* vol. 3, no. 1, pp. 38-45, 2012.

[37] M. Gholipour and H. Hashemipour, "Evaluation of multi-walled carbon nanotubes performance in adsorption and desorption of hexavalent chromium," *Chemical Industry & Chemical Engineering Quarterly,* vol. 19, no. 4, pp. 509-523, 2012.

[38] J. Zhu, S. Wei, H. Gu, S. Rapole, Q. Wang, Z. Luo, N. Haldolaarachchige, D. Young and Z. Guo, "One-Pot Synthesis of Magnetic Graphene Nanocomposites Decorated with Core@Double-shell Nanoparticles for Fast Chromium Removal," *Environmental Science & Technology,* vol. 46, no. 2, pp. 977-985, 2012.

[39] H. Qiu, L. Lv, B.-c. Pan, Q.-j. Zhang, W.-m. Zhang and Q.-x. Zhang, "Critical review in adsorption kinetic models," *Journal of Zhejiang University-SCIENCE A,* vol. 10, no. 5, pp. 716-724, 2009.

[40] S. Lyubchik, A. Lyubchik and O. Lygina, "Comparison of the Thermodynamic Parameters Estimation for the Adsorption Process of the Metals from Liquid

Phase on Activated Carbons," in *Thermodynamics - Interaction Studies - Solids, Liquids and Gases*, InTech, 2011.

[41] M. Anjum, R. Miandad, M. Waqas, F. Gehany and M. Barakat, "Remediation of wastewater using various nanomaterials," *Arabian Journal of Chemistry*, 2016.

[42] G. Z. Kyzas, "Adsorption in Wastewater Treatment," in *Green Adsorbents*, Bentham Science Publishers, pp. 35-53, 2015.

[43] B. Kakavandi, R. R. Kalantary, A. J. Jafari, S. Nasseri, A. Ameri, A. Esrafili and A. Azari, "Pb(II) Adsorption Onto a Magnetic Composite of Activated Carbon and Superparamagnetic Fe3O4 Nanoparticles: Experimental and Modeling Study," *Clean Soil Air Water*, vol. 43, no. 8, pp. 1157-1166, 2015.

[44] S. N. A. Abas, M. H. S. Ismail, S. I. Siajam and M. L. Kamal, "Development of novel adsorbent-mangrove-alginate composite bead (MACB) for removal of Pb(II) from aqueous solution," *Journal of the Taiwan Institute of Chemical Engineers*, vol. 50, no. 1, pp. 182-189, 2015.

[45] X. Wang, D. Shao, G. Hou, X. Wang, A. Alsaedi and B. Ahmad, "Uptake of Pb(II) and U(VI) ions from aqueous solutions by the ZSM-5 zeolite," *Journal of Molecular Liquids*, vol. 207, pp. 338-342, 2015.

[46] Y. Yu, J. G. Shapter, R. Popelka-Filcoff, J. W. Bennett and A. V. Ellisa, "Copper removal using bio-inspired polydopamine coated natural zeolites," *Journal of Hazardous Materials*, vol. 273, pp. 174-182, 2014.

[47] S. E. A. Sharaf El-Deen and G. E. Sharaf El-Deen, "Adsorption of Cr(VI) from Aqueous Solution by Activated Carbon Prepared from Agricultural Solid Waste," *Separation Science and Technology*, vol. 50, no. 10, pp. 1469-1479, 2015.

[48] Q. Liu, B. Y. Yang, L. Zhang and R. Huang, "Adsorptive removal of Cr(VI) from aqueous solutions by cross-linked chitosan/bentonite composite," *Korean Journal of Chemical Engineering*, vol. 32, no. 7, pp. 1314-1322, 2015.

[49] B. Qui, Y. Wang, D. Sun, Q. Wang, X. Zhang, B. L. Weeks, R. O'Connor, X. Huang, S. Wei and Z. Guo, "Cr(VI) removal by magnetic carbon nanocomposites derived from cellulose at different carbonization

temperatures," *Journal of Material Chemistry A,* vol. 3, no. 18, pp. 9817-9825 , 2015.

[50] B. Qiu, C. Xu, D. Sun, H. Yi, J. Guo, X. Zhang, H. Qu, M. Guerrero, X. Wang, N. Noel, Z. Luo, Z. Guo and S. Wei, "Polyaniline coated ethyl cellulose with improved hexavalent chromium removal," *ACS Sustain Chem Eng,* vol. 2, no. 8, pp. 2070-2080, 2014.

[51] K. Fujiwara, A. Ramesh, T. Maki, H. Hasegawa and K. Ueda, "Adsorption of platinum (IV), palladium (II) and gold (III) from aqueous solutions onto l-lysine modified crosslinked chitosan resin," *Journal of Hazardous Metals,* vol. 146, no. 1-2, pp. 39-50, 2007.

[52] G. Rivas, M. Rubianes, M. Pedano, N. Ferreyra, G. Luque and S. Miscoria, *Carbon Nanotubes: A New Alternative for Electrochemical Sensors,* Nova Science Publishers, Incorporated, 2009.

[53] R. Sitko, B. Zawisza and E. Malicka, "Modification of carbon nanotubes for preconcentration, separation and determination of trace-metal ions," *TrAC Trends in Analytical Chemistry,* vol. 37, pp. 22-31, 2012.

[54] M. Jian, H. Xie, K. Xia and Y. Zhang, "Challenge and Opportunities of Carbon Nanotubes," in *Industrial Applications of Carbon Nanotubes,* Beijing, Elsevier Inc., pp. 434-465, 2017.

[55] K. Pyrzyńska and M. Bystrzejewski, "Comparative study of heavy metal ions sorption onto activated carbon, carbon nanotubes, and carbon-encapsulated magnetic nanoparticles," *Colloids and Surfaces A: Physicochemical and Engineering Aspects,* vol. 362, no. 1-3, pp. 102-109, 2010.

[56] G. Purnachadra Rao, C. Lu and F. Su, "Sorption of divalent metal ions from aqueous solution by carbon nanotubes: a review," *Separation and Purification Technology,* vol. 58, no. 1, pp. 224-231, 2007.

[57] K. Pyrzynska, "Application of carbon sorbents for the concentration and separation of metal ions," *Analytical Sciences,* vol. 23, no. 6, pp. 631-637, 2007.

[58] M. Valcárcel, S. Cárdenas, B. Simonet, Y. Moliner-Martínez and R. Lucena, "Carbon nanostructures as sorbent materials in analytical processes," *TrAC Trends in Analytical Chemistry,* vol. 24, no. 1, pp. 34-43, 2008.

[59] M. Tuzen, K. Saygi and M. Soylak, “Solid phase extraction of heavy metal ions in environmental samples on multiwalled carbon nanotubes,” *Journal of Hazardous Materials,* vol. 2, no. 152, pp. 632-639, 2008.

[60] J. Muñoz, M. Gallego and M. Valcárcel, “Speciation of organometallic compounds in environmetal samples by gas chromatography after flow preconcentration on fullerenes and nanotubes,” *Analytical Chemistry,* vol. 77, no. 16, pp. 5389-5395, 2005.

[61] W. Liang, R. Xu, Y. Chen and R. Jiang, “Activity and stability comparison of immobilized NADH oxidase on multi-walled carbon nanotubes, carbon nanospheres, and single-walled carbon nanotubes,” *Journal of Molecular Catalysis B: Enzymatic,* vol. 69, no. 3-4, pp. 120-126, 2011.

[62] A. Eatemadi, H. Daraee, H. Karimkhanloo, M. Kouhi, . N. Zarghami, A. Akbarzadeh, M. Abasi, Y. Hanifehpour and S. Woo Joo, “Carbon nanotubes: properties, synthesis, purification, and medical applications,” *Nanoscale Research Letters,* vol. 393, no. 9, 2014.

[63] M. M. Rahman, S. A. Sime, M. A. Hossain, M. Shammi, M. K. Uddin, M. T. Sikder and M. Kurasaki, “Removal of Pollutants from Water by Using Single-Walled Carbon Nanotubes (SWCNTs) and Multi-walled Carbon Nanotubes (MWCNTs),” *Arabian Journal for Science and Engineering,* vol. 42, no. 1, pp. 261-269, 2017.

[64] P. Lambin and V. Popov, Carbon Nanotubes: *From Basic Research to Nanotechnology*, Sozopol, Bulgaria: Springer, 2006.

[65] A. Jorio, G. Dresselhaus and M. S. Dresselhaus, *Carbon Nanotubes: Advanced Topics in the Synthesis, Structure, Properties and Applications*, vol. 111, Springer Science & Business Media, 2007.

[66] E. Joselevich, H. Dai, J. Liu, K. Hata and A. H. Windle, *Carbon Nanotube Synthesis and Organization*, Berlin, Heidelberg: Springer, 2008, pp. 101-164.

[67] F. V. Ferreira, L. D. Cividanes, F. S. Brito, B. R. C. de Menezes, W. Franceschi, E. A. Simonetti and G. P. Thim, *Functionalization of Carbon Nanotube and Applications*, Springer, Cham, pp. 31-61, 2016.

[68] B. Arash, Q. Wang and V. Varadan, “Mechanical properties of carbon nanotube/polymer composites,” *Scientific Reports,* vol. 4, no. 6479, 2014.

[69] J.-P. Salvetat, J.-M. Bonard, N. Thomson, A. Kulik, L. Forr´o, W. Benoit and L. Zuppiroli, "Mechanical properties of carbon nanotubes," *Applied Physics A,* vol. 69, pp. 255-260, 1999.

[70] M. Abdel Salama and R. M. Mohameda, "Removal of antimony (III) by multi-walled carbon nanotubes from model solution and environmental samples," *Chemical Engineering Research and Design,* vol. 91, no. 7, pp. 1352-1360, 2013.

[71] H. Al-Johani and M. Abdel Salam, "Kinetics and thermodynamic study of aniline adsorption by multi-walled carbon nanotubes from aqueous solution," *Journal of Colloid and Interface Science,* vol. 360, no. 2, pp. 760-767, 2011.

[72] M. Abdel Salam, M. Mokhtar, S. Basahel, S. Al-Thabaiti and A. Obaid, "Removal of chlorophenol from aqueous solutions by multi-walled carbon nanotubes: Kinetic and thermodynamic studies," *Journal of Alloys and Compounds,* vol. 500, no. 1, pp. 87-92, 2010.

[73] J. Wang, X. Ma, G. Fang, M. Pan, X. Ye and S. Wang, "Preparation of iminodiacetic acid functionalized multi-walled carbon nanotubes and its application as sorbent for separation and preconcentration of heavy metal ions," *Journal of Hazardous Materials,* vol. 186, no. 1, pp. 1985-1992, 2011.

[74] N. V. Perez-Aguilar, E. Muñoz-Sandoval, P. E. Diaz-Flores and J. R. Rangel-Mendez, "Adsorption of cadmium and lead onto oxidized nitrogen-doped multiwall carbon nanotubes in aqueous solution: equilibrium and kinetics," *Nanoparticle Research,* vol. 12, no. 2, pp. 467-480, 2010.

[75] N. V. Perez-Aguilar, P. E. Diaz-Flores and J. R. Rangel-Mendez, "The adsorption kinetics of cadmium by three different types of carbon nanotubes," *Journal of Colloid and Interface Science,* vol. 364, no. 2, pp. 279-287, 2011.

[76] Z.-n. Huang, X.-l. Wang and D.-s. Yang, "Adsorption of Cr(VI) in wastewater using magnetic multi-wall carbon nanotubes," *Water Science and Engineering,* vol. 3, no. 8, pp. 226-232, 2015.

[77] C. Luo, Z. Tian, B. Yang, L. Zhang and S. Yan, "Manganese dioxide/iron oxide/acid oxidized multi-walled carbon nanotube magnetic nanocomposite for enhanced hexavalent chromium removal," *Chemical Engineering Journal,* vol. 234, pp. 256-265, 2013.

[78] C. Jung, J. Heo, J. Han, N. Her, S.-J. Lee, J. Oh, J. Ryu and Yoon, “Hexavalent chromium removal by various adsorbents: Powdered activated carbon, chitosan, and single/multi-walled carbon nanotubes,” *Separation and Purification Technology,* vol. 106, pp. 63-71, 2013.

[79] EPA, “Chromium, Hexavalent (Colorimetric),” EPA, 1992.

[80] G-Biosciences, “Safety Data Sheet,” in *CTAB,* vol. 7, St Louis, MO: G-Biosciences, 2016.

[81] S. A. Elfeky, S. E. Mahmoud and A. F. Youssef, “Applications of CTAB modified magnetic nanoparticles for removal of chromium (VI) from contaminated water,” *Journal of Advanced Research,* vol. 8, no. 4, pp. 435-445, 2017.

[82] T. Sathvika, A. Soni, K. Sharma, M. Praneeth, M. Mudaliyar, V. Rajesh and N. Rajesh, “Potential Application of Saccharomyces cerevisiae and Rhizobium Immobilized in Multi Walled Carbon Nanotubes to adsorb Hexavalent Chromium,” Scientific Reports, 2018.

[83] M. Yusuf, M. A. Khan, M. Otero, E. Abdullah, M. Hosomi, A. Terada and S. Riya, “Synthesis of CTAB intercalated graphene and its application for the adsorption of AR265 and AO7 dyes from water,” *Journal of Colloid and Interface Science,* vol. 493, pp. 51-61, 2017.

[84] L. Anah and N. Astrini, “Influence of pH on Cr(VI) ions removal from aqueous solutions using carboxymethyl cellulose-based hydrogel as adsorbent,” in *IOP Conference Series: Earth and Environmental Science*, Jalan Cisitu 21/154 D, Bandung 40135, Indonesia, 2017.

[85] D. Zhang, Y. Ma, ,. H. Feng and Y. Hao, “Adsorption Of Cr(VI) from Aqueous Solution using Carbon-Microsilica composite Adsorbent,” *Journal of the Chilean Chemical Society,* vol. 57, pp. 964-968, 2012.

[86] J. Dai, F. Ren and C. Tao, “Adsorption of Cr(VI) and Speciation of Cr(VI) and Cr(III) in Aqueous Solutions Using Chemically Modified Chitosan,” *International Journal of Environmental Research and Public Health,* vol. 9, no. 5, pp. 1757-1770, 2012.

[87] H. Beheshti, M. Irani, L. Hosseini, A. Rahimi and M. Aliabadi, “Removal of Cr (VI) from aqueous solutions using chitosan/MWCNT/Fe3O4 composite

nanofibers-batch and column studies," *Chemical Engineering Journal,* vol. 284, pp. 557-564, 2016.

[88] S. Sambaza, M. Masheane, S. Malinga, E. Nxumalo and S. Mhlanga, "Polyethyleneimine-carbon nanotube polymeric nanocomposite adsorbents for the removal of Cr6+ from water," *Physics and Chemistry of the Earth, Parts A/B/C,* vol. 100, pp. 236-246, 2017.

[89] J. Hu, C. Chen, X. Zhu and X. Wang, "Removal of chromium from aqueous solution by using oxidized oxidized multiwalled carbon nanotubes," *Journal of Hazardous Materials,* vol. 162, no. 2-3, pp. 1542-1550, 2009.

[90] L. Largittea and R. Pasquier, "A review of the kinetics adsorption models and their application to the adsorption of lead by an activated carbon," *Chemical Engineering Research and Design,* vol. 109, pp. 495-504, 2016.

[91] Y. Liu and J. Wang, *Fundamentals and Applications of Biosorption Isotherms, Kinetics and Thermodynamics,* Nova Science Publishers, 2009.

[92] A. Ghaedi, M. Ghaedi, A. Pouranfard, A. Ansari, Z. Avazzadeh, A. Vafaei, I. Tyagi, S. Agarwal and V. K. Gupta, "Adsorption of Triamterene on multi-walled and single-walled carbon nanotubes: Artificial neural network modeling and genetic algorithm optimization," *Journal of Molecular Liquids,* vol. 216, pp. 654-665, 2016.

Vita

Tamara Dokmaji was born in 1994, in Sharjah, United Arab Emirates. She received her primary and secondary education in Dubai, UAE. She received her B.Sc. degree in Chemical Engineering from the American University of Sharjah in 2016. From 2016 she began her career and worked as an Assistant Engineer in Asset Integrity Engineering.

In September 2016, she joined the Chemical Engineering master's program in the American University of Sharjah as a full-time student. Her research interests are in areas of water and wastewater treatment, biofuels, sustainability, and reaction modelling.